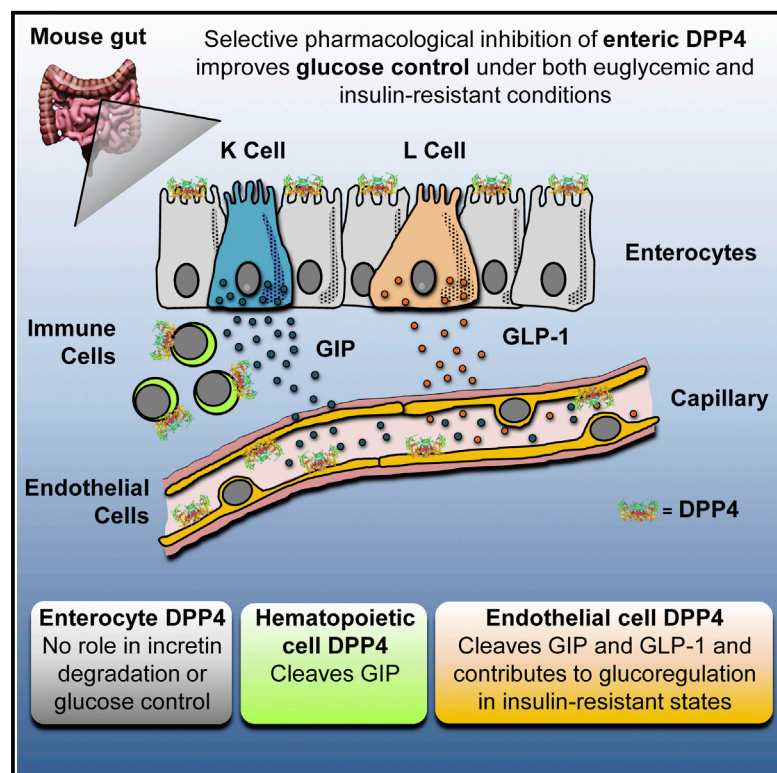


Cell Metabolism

Cellular Sites and Mechanisms Linking Reduction of Dipeptidyl Peptidase-4 Activity to Control of Incretin Hormone Action and Glucose Homeostasis

Graphical Abstract



Authors

Erin E. Mulvihill, Elodie M. Varin, Bojana Gladanac, ..., K.W. Annie Bang, Julio E. Ayala, Daniel J. Drucker

Correspondence

drucker@lunenfeld.ca

In Brief

Mulvihill et al. show that, although a substantial amount of DPP4 is produced by enterocytes, it is the endothelial cell-derived DPP4 that contributes to plasma DPP4 activity and glucose metabolism. Unexpectedly, bone marrow-derived DPP4 selectively inactivates GIP but not GLP-1.

Highlights

- Endothelial-derived DPP4 controls the enteroinsular incretin axis
- DPP4 expressed by hematopoietic cells selectively regulates cleavage of GIP
- DPP4 in villin⁺ gut epithelium is dispensable for incretin-mediated gluco-regulation



Cellular Sites and Mechanisms Linking Reduction of Dipeptidyl Peptidase-4 Activity to Control of Incretin Hormone Action and Glucose Homeostasis

Erin E. Mulvihill,^{1,6} Elodie M. Varin,^{1,6} Bojana Gladanac,¹ Jonathan E. Campbell,^{1,8} John R. Ussher,^{1,7} Laurie L. Baggio,¹ Bernardo Yusta,¹ Jennifer Ayala,³ Melissa A. Burmeister,³ Dianne Matthews,¹ K.W. Annie Bang,^{1,4,5} Julio E. Ayala,³ and Daniel J. Drucker^{1,2,9,*}

¹Lunenfeld-Tanenbaum Research Institute, Mt. Sinai Hospital, Toronto, ON M5G 1X5, Canada

²Department of Medicine, University of Toronto, Toronto, ON M5S 2J7, Canada

³Sanford Burnham Prebys Medical Discovery Institute at Lake Nona, Center for Metabolic Origins of Disease, Orlando, FL 32827, USA

⁴Division of Reproductive Sciences, University of Toronto, Toronto, ON M5S 2J7, Canada

⁵Institute of Medical Sciences, University of Toronto, Toronto, ON M5S 2J7, Canada

⁶Co-first author

⁷Present address: Faculty of Pharmacy and Pharmaceutical Sciences, University of Alberta, Edmonton, AB T6G 2E1, Canada

⁸Present address: Duke University Molecular Physiology Institute, 50-104, 300 N Duke Street, Durham, NC 27701, USA

⁹Lead Contact

*Correspondence: drucker@lunenfeld.ca

<http://dx.doi.org/10.1016/j.cmet.2016.10.007>

SUMMARY

Pharmacological inhibition of the dipeptidyl peptidase-4 (DPP4) enzyme potentiates incretin action and is widely used to treat type 2 diabetes. Nevertheless, the precise cells and tissues critical for incretin degradation and glucose homeostasis remain unknown. Here, we use mouse genetics and pharmacologic DPP4 inhibition to identify DPP4⁺ cell types essential for incretin action. Although enterocyte DPP4 accounted for substantial intestinal DPP4 activity, ablation of enterocyte DPP4 in *Dpp4*^{Gut-/-} mice did not produce alterations in plasma DPP4 activity, incretin hormone levels, and glucose tolerance. In contrast, endothelial cell (EC)-derived DPP4 contributed substantially to levels of soluble plasma DPP4 activity, incretin degradation, and glucose control. Surprisingly, DPP4⁺ cells of bone marrow origin mediated the selective degradation of fasting GIP, but not GLP-1. Collectively, these findings identify distinct roles for DPP4 in the EC versus the bone marrow compartment for selective incretin degradation and DPP4i-mediated glucoregulation.

INTRODUCTION

Type 2 diabetes mellitus (T2DM) is a metabolic disorder characterized by impaired insulin action and islet cell dysfunction (insufficient insulin and excess glucagon secretion) resulting in hyperglycemia. Among the newer antidiabetic agents used to treat subjects with T2DM, both glucagon-like peptide-1 receptor agonists (GLP-1RA) and dipeptidyl peptidase-4 inhibitors (DPP4i) potentiate gut hormone action (Campbell and Drucker, 2013; Drucker and Nauck, 2006; Inzucchi et al., 2012). GLP-

1RAs are injectable, often peptide-based agents that circulate systemically and interact with a single, well-defined GLP-1R. In contrast, DPP4i are small molecule, orally ingested enzyme inhibitors that are better tolerated and, hence, more widely prescribed. Although the GLP-1R is the primary target for the glucoregulatory actions of GLP-1R agonists (Campbell and Drucker, 2013; Lamont et al., 2012; Smith et al., 2014; Tatarkiewicz et al., 2014), the precise tissues, molecular targets, and signaling pathways critical for transducing the glucoregulatory actions of DPP4i remain incompletely understood.

DPP4 is a widely expressed exopeptidase that exists in two principal isoforms: a membrane-anchored enzyme containing a short intracellular tail and a soluble (sDPP4) circulating form; interestingly both isoforms display enzymatic activity (Mulvihill and Drucker, 2014). DPP4 has over 40 identified substrates, however, the principal targets for glucoregulation are GLP-1 and glucose-dependent insulinotropic polypeptide (GIP) (Flock et al., 2007; Hansotia et al., 2004; Mulvihill and Drucker, 2014; Omar and Ahrén, 2014). Both GLP-1 and GIP are secreted from enteroendocrine cells at low basal rates in the fasting state and their plasma levels increase post-prandially. Circulating levels of intact, bioactive incretin hormones are extremely low due to rapid inactivation by DPP4 and renal clearance (Campbell and Drucker, 2013; Nauck and Meier, 2016; Sandoval and D'Alessio, 2015).

Within the gut, three cell types are considered the principal sites of DPP4 expression and activity: enterocytes, cells of hematopoietic origin, and vascular endothelial cells (Hansen et al., 1999; Mulvihill and Drucker, 2014). Notably, these cell types are all situated in proximity to enteroendocrine cells, rendering them highly suited anatomically for the DPP4-dependent control of peptide hormone degradation (Hansen et al., 1999). As a result, the majority of GLP-1 and GIP is degraded rapidly following secretion, and the DPP4-generated metabolites of GLP-1 and GIP are not high-affinity agonists for their classical receptors (Campbell and Drucker, 2013; Deacon et al., 1995; Hansen et al., 1999; Rolin et al., 2004). Hence, whether the glucoregulatory actions of endogenous incretin hormones

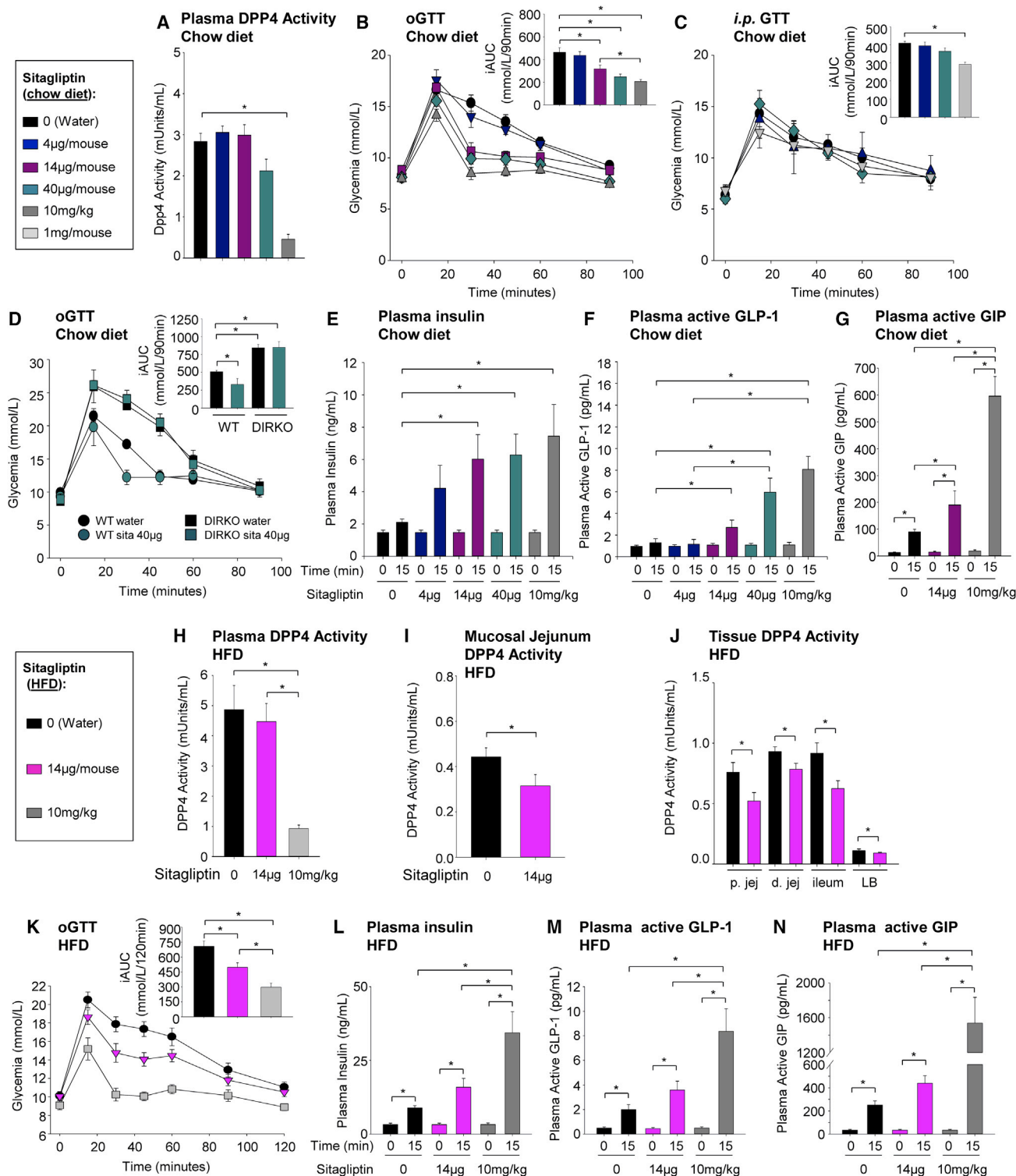


Figure 1. Acute Dosing of Low Concentrations of Sitagliptin Regulates Glucose Metabolism in Chow- and High Fat Diet-Fed Wild-Type Mice

(A) Plasma DPP4 activity 30 min after sitagliptin or water gavage in fasted WT mice fed a regular chow diet ($n = 4-7$ mice/group).

(B and C) Blood glucose taken 0–90 min after oral (B) or intraperitoneal (C) administration of glucose in 10-week-old WT mice treated with sitagliptin. Inset depicts calculated incremental area under the curve (iAUC) for glucose excursions ($n = 10-15$ /group).

(D) Blood glucose taken 0–90 min after administration of oral glucose in 10-week-old WT or DIRKO mice treated with 40 μ g/mouse sitagliptin. Insets depict iAUC for glucose excursions ($n = 5$ /group).

(legend continued on next page)

are predominantly mediated via circulating intact peptides and classical endocrine mechanisms or through signals arising locally in the gut and propagated through neural and/or paracrine mechanisms remains unclear (Burcelin et al., 2014; Sandoval and D'Alessio, 2015; Waget et al., 2011).

Experiments using low concentrations of DPP4i (that do not affect systemic DPP4 activity) have identified the gastrointestinal tract as a major site of action for the acute glucoregulatory actions of DPP4i in normoglycemic mice (Waget et al., 2011). However, the precise cellular targets, within or beyond the gut, important for transducing the acute and chronic metabolic actions emanating from reduced DPP4 activity in normoglycemic or dysglycemic mice remain uncertain. To elucidate the importance of enterocyte versus endothelial versus bone marrow-derived DPP4 for control of the enteroinsular axis, we generated and analyzed mice with: (1) elimination of *Dpp4* in enterocytes (*Dpp4*^{Gut^{-/-}), (2) elimination of DPP4 in both endothelial and hematopoietic cells (*Dpp4*^{EC^{-/-}), and (3) elimination of DPP4 specifically in endothelial cells (*Dpp4*^{EC^{-/-} mice reconstituted with bone marrow from wild-type (WT) donor mice (*Dpp4*^{EC^{-/-} (BMT)).}}}}

RESULTS

Enteral Inhibition of DPP4 Is Sufficient to Regulate Glucose Metabolism in Chow- and High Fat Diet-Fed Wild-Type Mice

We first re-assessed previous observations linking intestinal selective sitagliptin treatment with improvement of oral glucose tolerance independent of changes in plasma DPP4 activity (Waget et al., 2011). Although high dose sitagliptin (10 mg/kg body weight, referenced as systemic inhibition) robustly lowered plasma DPP4 activity (Figure 1A) and improved oral glucose tolerance (Figure 1B), selective enteral inhibition of DPP4 activity with low dose sitagliptin (14 μg/mouse, referenced as intestinal-selective inhibition) significantly improved oral glucose tolerance (Figure 1B) without affecting plasma DPP4 activity (Figure 1A). In contrast to findings with systemic DPP4 inhibition, intestinal-selective inhibition of DPP4 activity with sitagliptin did not reduce glycemic excursion during an intraperitoneal glucose tolerance test (i.p. GTT) (Figure 1C). The glucoregulatory actions of intestinal-selective inhibition of DPP4 with sitagliptin were absent in mice lacking both the *Glp1r* and *Gipr* (double incretin receptor knockout [DIRKO]) (Figure 1D). Notably, intestinal-selective DPP4 inhibition with sitagliptin increased insulin levels (Figure 1E), as well as plasma levels of intact GLP-1 and GIP (Figures 1F and 1G). None of the concentrations of sitagliptin inhibited gastric emptying (Figure S1).

As previous studies assessed metabolic effects of intestinal-selective DPP4 inhibition predominantly in normoglycemic

mice (Waget et al., 2011), we examined the actions of sitagliptin in high fat diet (HFD)-fed mice. Intestinal-selective DPP4 inhibition (14 μg/mouse) did not reduce plasma DPP4 activity in mice fed a HFD (Figure 1H). However, DPP4 activity in jejunal mucosa (Figure 1I) and in whole gut extracts from both the small and large bowel (Figure 1J) was reduced after intestinal-selective DPP4 inhibition with sitagliptin. Moreover, glycemic excursions were lower after an oral glucose challenge (Figure 1K), and plasma levels of insulin, active GLP-1, and active GIP were unchanged (versus control) after intestinal-selective DPP4 inhibition with sitagliptin (Figures 1L–N). In contrast, systemic inhibition of DPP4 with 10 mg/kg sitagliptin significantly increased circulating levels of insulin and active incretin hormones in HFD-fed mice (Figures 1L–1N).

Dpp4^{Gut^{-/-}} Mice Exhibit Markedly Reduced Intestinal DPP4 Activity, but No Improvement in Glucose Tolerance

To more precisely delineate the cellular target(s) of DPP4i within the gut, we generated mice with selective inactivation of *Dpp4* in enterocytes (*Dpp4*^{Gut^{-/-}; Figure 2A). Levels of *Dpp4* mRNA transcripts in gut extracts and mucosa were 90% lower throughout the length of the intestine from *Dpp4*^{Gut^{-/-} versus control *Vil-Cre* mice, whereas *Dpp4* expression in liver, kidney, and spleen was not reduced (Figures 2B and 2C). Consistent with the RNA data, DPP4 enzyme activity was markedly reduced in gut extracts (Figure 2D) and mucosal scrapings (Figure 2E) from intestinal segments of *Dpp4*^{Gut^{-/-} mice, whereas plasma DPP4 activity was not different compared to *Vil-Cre* controls (Figure 2F). Surprisingly, despite marked reduction of intestinal mucosal DPP4 activity in *Dpp4*^{Gut^{-/-} mice, oral glucose tolerance and insulin levels were unchanged (Figures 2G and 2H). Plasma levels of active GLP-1 were not increased (Figure 2I), whereas the rise in post-prandial active GIP was reduced in *Dpp4*^{Gut^{-/-} versus *Vil-Cre* control mice (Figure 2J). Furthermore, intestinal-selective DPP4 inhibition continued to produce a modest yet significant reduction in glycemic excursion after oral glucose administration in *Dpp4*^{Gut^{-/-} (Figures 2K–2M), and both *Dpp4*^{Gut^{-/-} and *Vil-Cre* control mice responded similarly to intestinal-selective DPP4 inhibition with equivalent increases in plasma insulin, active GLP-1, and active GIP levels (Figures S2A–S2C). After 8 weeks of HFD feeding, *Dpp4*^{Gut^{-/-} mice exhibited similar body weights and food intake compared to *Vil-Cre* controls (Figures S2D–S2F). Consistent with findings in chow-fed *Dpp4*^{Gut^{-/-} mice, oral glucose tolerance and insulin levels were similar between the two groups, and active levels of incretins were not preferentially increased following sitagliptin administration in HFD-fed *Dpp4*^{Gut^{-/-} versus control mice (Figures S2G–S2L). Taken together, these findings reveal that}}}}}}}}}}

(E–G) Plasma insulin (E), active GLP-1 (F), and active GIP (G) measured at 0 and 15 min after glucose challenge (45 min after sitagliptin/water gavage) during an OGTT in 10- to 12-week-old WT mice (n = 6–13/group).

(H) Plasma DPP4 activity 30 min after sitagliptin or water gavage in WT mice fed a HFD for 4 weeks (n = 5–15 mice/group).

(I and J) DPP4 activity in mucosal scrapings or in extracts isolated from whole intestinal tissues from mice treated 30 min prior with 14 μg of sitagliptin (n = 7–9/group).

(K) Blood glucose taken 0–120 min after administration of oral glucose in 19- to 22-week-old WT mice fed a HFD for 4–6 weeks and treated with 14 μg/mouse or 10 mg/kg sitagliptin. Inset depicts iAUC analysis for glucose excursions (n = 16–17 mice/group).

(L–N) Plasma insulin (L), active GLP-1 (M), and active GIP (N) measured at 0 and 15 min after glucose gavage during an OGTT in HFD-fed WT mice (n = 5–11/group). Data are presented as the mean ± SEM. *p ≤ 0.05.

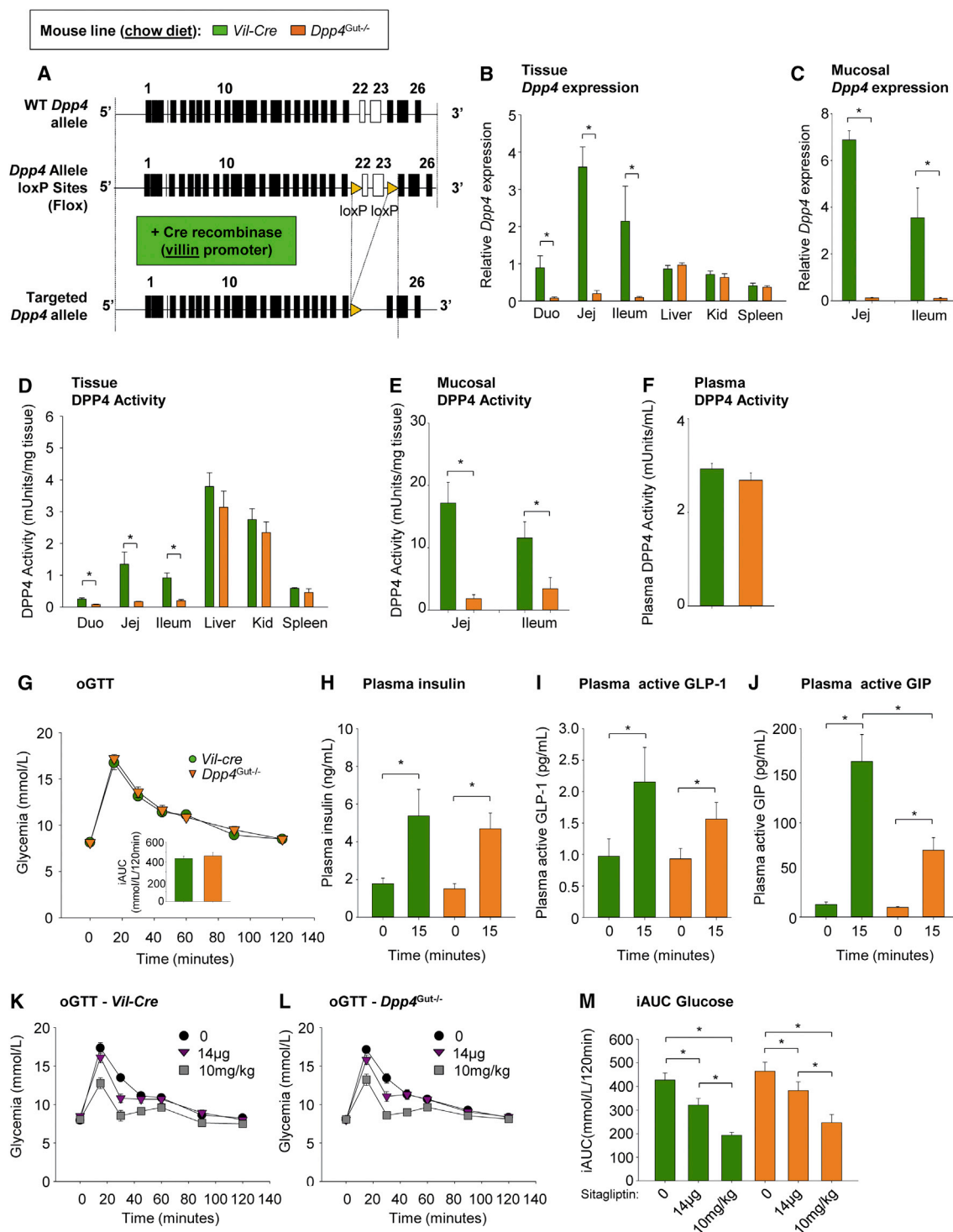


Figure 2. Disruption of *Dpp4* in Villin⁺ Cells of the Gut Epithelium Does Not Perturb the Enteroinsular Axis

(A) Schematic of Cre LoXP targeting strategy for *Dpp4* to generate tissue-specific knockouts.

(B and C) mRNA abundance of *Dpp4* normalized to *Ppia* in whole extracts (B) of intestinal segments (Duo, duodenum; Jej, jejunum and ileum), liver (Liv), kidney (Kid), and spleen tissue or mucosal scrapings (C) of chow-fed 6- to 10-week-old female mice (n = 3–8/group).

(D and E) DPP4 activity in extracts made from whole tissue (D) or mucosal scrapings (E) isolated from intestine, and whole extracts isolated from liver, kidney, and spleen (D) of chow-fed mice 6- to 10-week-old female mice (n = 3–8/group).

(F) Plasma DPP4 activity in *Dpp4^{Gut-/-}* and *Vil-cre* control fed on chow diet.

(legend continued on next page)

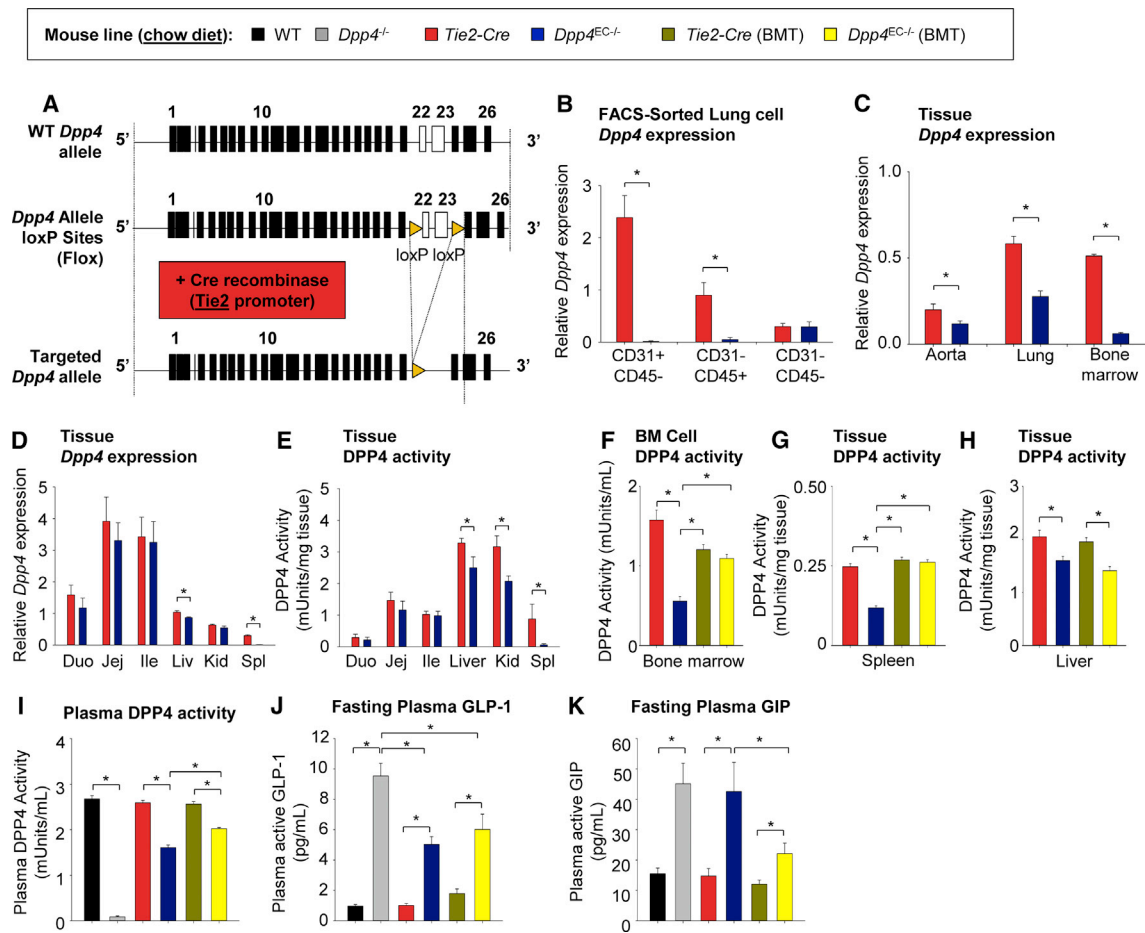


Figure 3. *Dpp4^{EC-/-}* and *Dpp4^{EC-/-}* (BMT) Mice Exhibit Reduced Plasma DPP4 Activity and Increased Incretin Levels

(A) Schematic of Cre LoXP targeting of *Dpp4* to generate tissue-specific knockouts.

(B–D) mRNA abundance of *Dpp4* normalized to *Ppia* in cells isolated from lung and sorted by flow cytometry (B) or whole extracts of aorta, lung, bone marrow (C), or intestinal segments (duodenum, [Duo], jejunum [Jej], and ileum) [Ile], liver (Liv), kidney (Kid), and spleen tissue (D) ($n = 4–10$ /group).

(E) DPP4 activity in whole tissue extracts from intestinal segments, liver, kidney, and spleen of chow-fed female mice ($n = 3–4$ /group).

(F–H) DPP4 activity in bone marrow (BM), spleen and liver of 40- to 44-week-old *Dpp4^{EC-/-}* without bone marrow transplant or 30 weeks post-bone marrow transplant after 14 weeks of HFD feeding ($n = 7–8$ /group).

(I–K) Plasma DPP4 activity (I) ($n = 8–30$ mice/group), active GLP-1 (J), and active GIP (K) ($n = 8–18$ /group) in 5 hr-fasted controls or *Dpp4*-targeted chow-diet fed mice. Data are means \pm SEM. * $p \leq 0.05$.

elimination of DPP4 in the gut epithelium targeted by *Vil-Cre* is not sufficient to recapitulate the metabolic phenotypes observed in *Dpp4^{-/-}* mice (Conarello et al., 2003; Marguet et al., 2000) or in WT mice with intestinal-selective DPP4 inhibition (Waget et al., 2011).

***Dpp4^{EC-/-}* and *Dpp4^{EC-/-}* (BMT) Mice Exhibit Reduced Plasma DPP4 Activity and Increased Incretin Levels**

To further identify cellular site(s) of DPP4 expression that transduce a glucoregulatory response to DPP4i, we inactivated

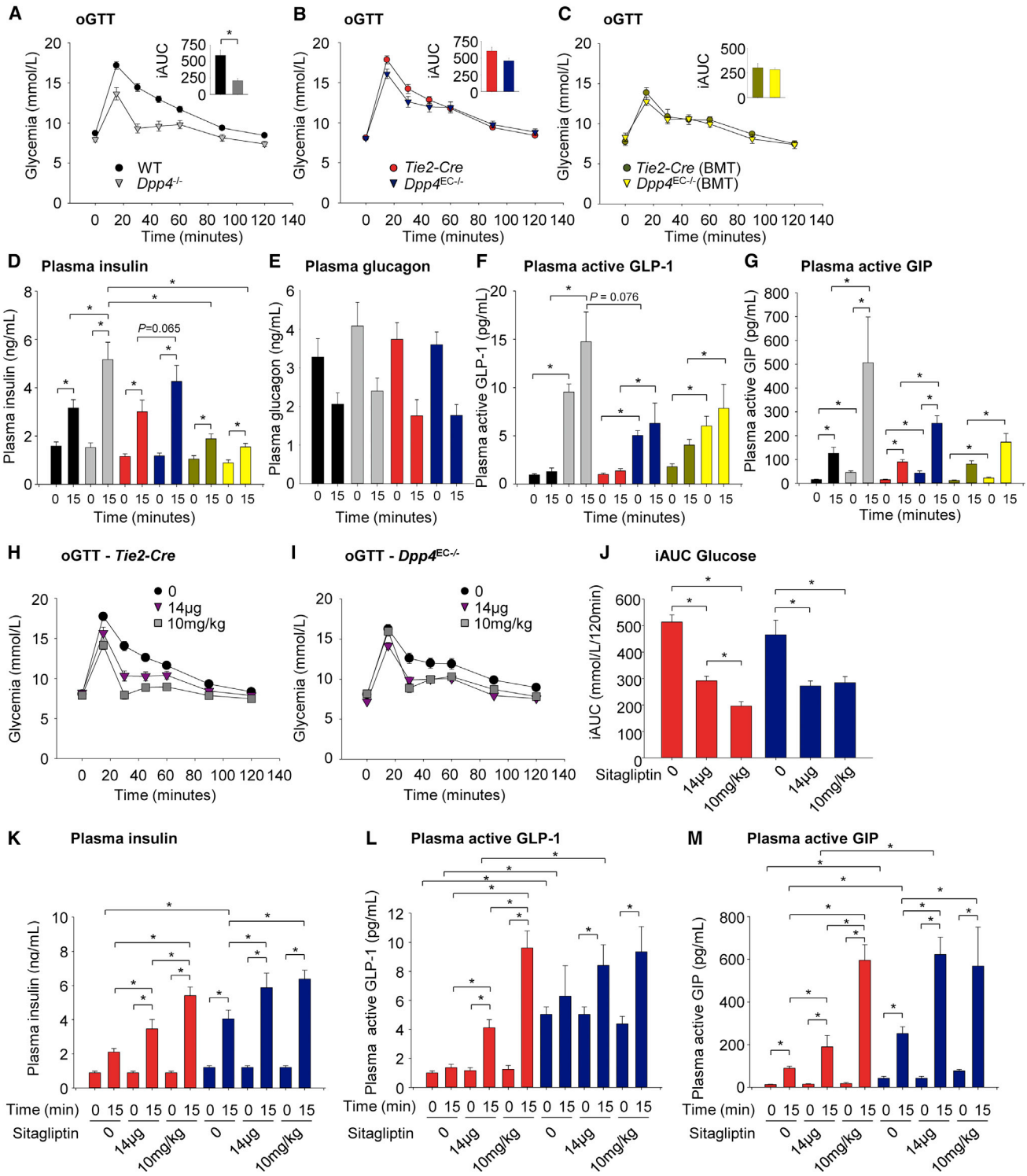
Dpp4 in hematopoietic and endothelial cells (*Dpp4^{EC-/-}*; Figure 3A) using the *Tie2* promoter to drive expression of Cre recombinase. Regular chow diet-fed *Tie2-Cre* mice did not differ significantly from WT mice or mice carrying the floxed *Dpp4* allele (Flox *Dpp4*) in regard to plasma DPP4 activity, glucose tolerance, and plasma insulin and incretin hormone levels (Figures S3A–S3G). These parameters were also similar in all three groups of mice after HFD feeding (Figures S3H–S3N). Therefore, we used *Tie2-Cre* mice as controls for all experiments. *Dpp4* expression was reduced by 95% in sorted CD31⁺

(G) Blood glucose taken 0–120 min after administration of oral glucose in mice fasted for 5–6 hr. Inset depicts iAUC analysis for glucose excursions ($n = 20–27$ /group).

(H–J) Plasma insulin (H), active GLP-1 (I), and active GIP (J) measured at 0 and 15 min after glucose challenge during an OGTT in control and *Dpp4^{Gut-/-}* mice ($n = 6–14$ /group).

(K–M) Blood glucose and area under the curve analysis taken 0–120 min after administration of oral glucose in control and *Dpp4^{Gut-/-}* mice treated with two doses of sitagliptin ($n = 9–27$ mice/group). Data are presented as the mean \pm SEM. * $p \leq 0.05$.

Mouse line (chow diet): ■ WT ■ *Dpp4*^{-/-} ■ *Tie2-Cre* ■ *Dpp4*^{EC/-} ■ *Tie2-Cre* (BMT) ■ *Dpp4*^{EC/-} (BMT)



(legend on next page)

lung endothelial cells from *Dpp4*^{EC-/-} mice (Figures 3B and S4A–S4C). Significant reductions in *Dpp4* mRNA expression were also observed in tissues rich in endothelial cells including the aorta and lung (Figure 3C). Consistent with the expression of the *Tie2* promoter in the hematopoietic cell lineage (Tang et al., 2010), *Dpp4* expression was reduced in CD45⁺ cells sorted from the lung (Figure 3B), as well as in the spleen (Figure 3D) and in bone marrow cells isolated from the femur and tibia (Figure 3C). In contrast, no changes in *Dpp4* expression were detected in CD45⁺ CD31⁻ cells (Figure 3B). Deletion of endothelial and hematopoietic cell *Dpp4* expression also accounted for a modest reduction in *Dpp4* mRNA abundance in the liver of *Dpp4*^{EC-/-} mice (Figure 3D), and DPP4 activity was reduced in liver, kidney, and spleen of *Dpp4*^{EC-/-} mice compared to *Tie2-Cre* controls (Figure 3E). Both *Dpp4* expression and DPP4 activity in whole gut tissue and mucosal scrapings were similar in *Dpp4*^{EC-/-} versus *Tie2-Cre* mice throughout the gut (Figures 3D, 3E, S4D, and S4E). As no differences in allocation of hematopoietic cell populations were detected in *Dpp4*^{EC-/-} versus *Tie2-Cre* mice (Figures S5A and S5B), we sought to discriminate the contribution of endothelial versus hematopoietic-derived DPP4 to the glucoregulatory response to sitagliptin. As such, we reconstituted irradiated control and *Dpp4*^{EC-/-} mice with congenic bone marrow (BM) from WT donor mice (designated as *Tie2-Cre*(BMT) and *Dpp4*^{EC-/-}(BMT), respectively). Donor chimerism, determined by flow cytometry 10 weeks after BM transplant, was 93% ± 0.45% in *Tie2-Cre*(BMT) and 94% ± 0.27% in *Dpp4*^{EC-/-}(BMT) as assessed in peripheral blood nucleated cells from recipient mice (Figures S5C–S5G). Upon receipt of donor bone marrow from WT mice, DPP4 activity was restored to a level similar to *Tie2-Cre*(BMT) in bone marrow and spleen of *Dpp4*^{EC-/-}(BMT) mice (Figures 3F and 3G). Consistent with hepatic endothelial cell content, DPP4 activity remained modestly reduced in liver from *Dpp4*^{EC-/-}(BMT) mice versus *Tie2-Cre*(BMT) controls (Figure 3H).

We next compared plasma DPP4 activity and plasma incretin levels in *Dpp4*^{-/-}, *Dpp4*^{EC-/-}, *Dpp4*^{EC-/-}(BMT), and control mice. In the fasting state, whole body disruption of the *Dpp4* gene resulted in almost undetectable plasma DPP4 activity (Figure 3I), as well as 10-fold and 3-fold elevations in levels of active GLP-1 and GIP, respectively (Figures 3J and 3K). In contrast, *Dpp4*^{EC-/-} mice exhibited an ~40%–50% reduction in plasma DPP4 activity (Figure 3I), a 5-fold elevation in active GLP-1 (~50% of what was observed for *Dpp4*^{-/-} mice; Figure 3J), and a 3-fold increase in levels of active GIP (similar to *Dpp4*^{-/-}, Figure 3K). Following bone marrow transplantation to rescue hematopoietic cell lineages in *Dpp4*^{EC-/-}(BMT) mice, plasma DPP4 activity remained significantly decreased by

~25% (Figure 3I). Interestingly, following BM reconstitution in *Dpp4*^{EC-/-}(BMT) mice, plasma levels of active GLP-1 remained elevated at levels similar to those detected in *Dpp4*^{EC-/-} mice (Figure 3J), indicating an important role for ECs, but not bone marrow-derived cells, in the control of GLP-1 degradation. In contrast, reconstitution of WT DPP4 activity in bone marrow of *Dpp4*^{EC-/-} mice reduced plasma fasting levels of active GIP relative to those detected in *Dpp4*^{EC-/-} and *Dpp4*^{-/-} mice (Figure 3K), revealing an unexpected essential role for hematopoietic cells in DPP4-dependent GIP inactivation.

Elevated Incretin Levels Are Not Sufficient to Improve Glucose Tolerance in *Dpp4*^{EC-/-} and *Dpp4*^{EC-/-}(BMT) Mice

We next compared the integrity of the enteroinsular axis in whole body *Dpp4*^{-/-}, *Dpp4*^{EC-/-}, *Dpp4*^{EC-/-}(BMT), and control mice. In accordance with previous studies (Marguet et al., 2000), regular chow-fed *Dpp4*^{-/-} mice exhibited an improved glucose excursion (Figure 4A), which was associated with a 1.5-fold increase in glucose-stimulated insulin levels and no change in suppression of glucagon compared with control mice (Figures 4D and 4E). Plasma levels of active GLP-1 and GIP were increased by 1.5- and 10-fold in *Dpp4*^{-/-} mice, respectively, in response to oral glucose (corresponding to concentrations approximately ten and four times higher than levels in WT mice, respectively) (Figures 4F and 4G). Surprisingly, *Dpp4*^{EC-/-} mice did not exhibit improved glucose tolerance (Figure 4B), despite elevations in plasma levels of insulin (similar to levels in *Dpp4*^{-/-} mice), and active GLP-1 and GIP (~50% of levels observed in *Dpp4*^{-/-} mice) in response to oral glucose (Figures 4D–4G). No differences in plasma glucagon were observed (Figure 4E). The two groups of mice irradiated and transplanted with WT bone marrow both exhibited improved glucose tolerance (Figure 4C versus 4A and 4B), and no deterioration of glucose tolerance or changes in levels of insulin or incretin hormones were detected following bone marrow transplantation in *Dpp4*^{EC-/-}(BMT) mice compared with *Tie2-Cre*(BMT) mice (Figures 4D–4G).

As short-term administration of DPP4i may improve insulin sensitivity independent of marked changes in glycemia (Uttschneider et al., 2008), we assessed insulin action in chow-fed, conscious, unrestrained control (*Flox Dpp4* and *Tie2-Cre*) and *Dpp4*^{EC-/-} mice using the hyperinsulinemic (2.5 mU/kg/min) euglycemic clamp. Arterial glucose was clamped at similar levels in both groups (Figure S6A), and the glucose infusion rate (GIR) necessary to maintain euglycemia was not different between groups (Figures S6B and S6C). However, both basal and clamp insulin levels were higher in *Dpp4*^{EC-/-} mice (Figure S6D), and

Figure 4. *Dpp4*^{EC-/-} and *Dpp4*^{EC-/-}(BMT) Mice Fail to Exhibit Improved Oral Glucose Tolerance and Retain Glucoregulatory Responses to Sitagliptin

(A–C) Blood glucose taken 0–120 min after administration of oral glucose in *Dpp4*-targeted mice fasted for 5–6 hr. Insets depict iAUC analysis of glucose excursions (n = 8–34 mice/group).

(D–G) Plasma insulin (D), glucagon (E), active GLP-1 (F), and active GIP (G) measured at 0 and 15 min after glucose challenge during an OGTT in control and *Dpp4*-targeted mice (n = 8–18/group).

(H–J) Blood glucose and iAUC analysis taken 0–120 min after administration of oral glucose in control and *Dpp4*^{EC-/-} mice treated with either 14 μg/mouse or 10 mg/kg sitagliptin and fed a regular chow diet (n = 15–27 mice/group).

(K–M) Plasma insulin (K), active GLP-1 (L), and active GIP (M) measured at 0 and 15 min after glucose challenge during an OGTT in *Dpp4*-targeted and control mice treated with 14 μg/mouse or 10 mg/kg sitagliptin and fed a chow diet (n = 6–12 mice/group). Data are presented as the mean ± SEM. *p < 0.05.

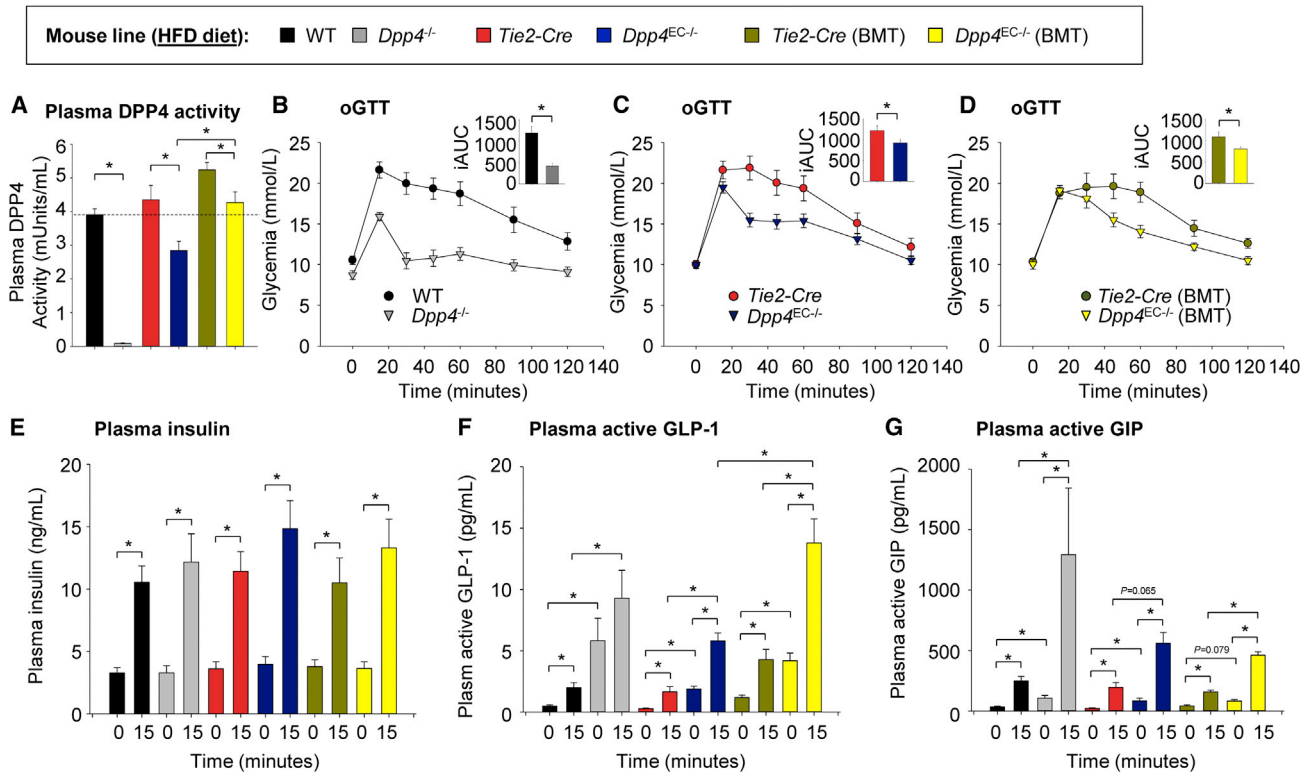


Figure 5. HFD-Fed $Dpp4^{EC-/-}$ and $Dpp4^{EC-/-}$ (BMT) Mice Are Protected from Glucose Intolerance in the Insulin-Resistant State

(A) Plasma DPP4 activity in 5 hr-fasted control and $Dpp4$ -targeted mice after 8 weeks of HFD ($n = 8-21$).

(B-D) Oral glucose tolerance in $Dpp4$ -targeted and control mice fasted for 5-6 hr and fed a HFD for 4-6 weeks. Insets depict iAUC analysis of glucose excursions ($n = 8-27$ mice/group).

(E-G) Plasma insulin (E), active GLP-1 (F), and active GIP (G) measured at 0 and 15 min after glucose challenge ($n = 5-12$ /group). Data are means \pm SEM. * $p \leq 0.05$.

insulin-mediated suppression of endoR_a (glucose appearance) was greater in $Dpp4^{EC-/-}$ compared to control mice (Figure S6E). Conversely, despite higher clamped insulin levels, stimulation of R_d (glucose disposal) was impaired in $Dpp4^{EC-/-}$ compared to control mice (Figures S6F-S6L). Altogether, these data indicate that under a chow diet, $Dpp4^{EC-/-}$ mice have no improvement in glucose tolerance and reduced insulin sensitivity in tissues utilizing glucose.

Chow-Fed $Dpp4^{EC-/-}$ Mice Retain Glucoregulatory Sensitivity to Sitagliptin

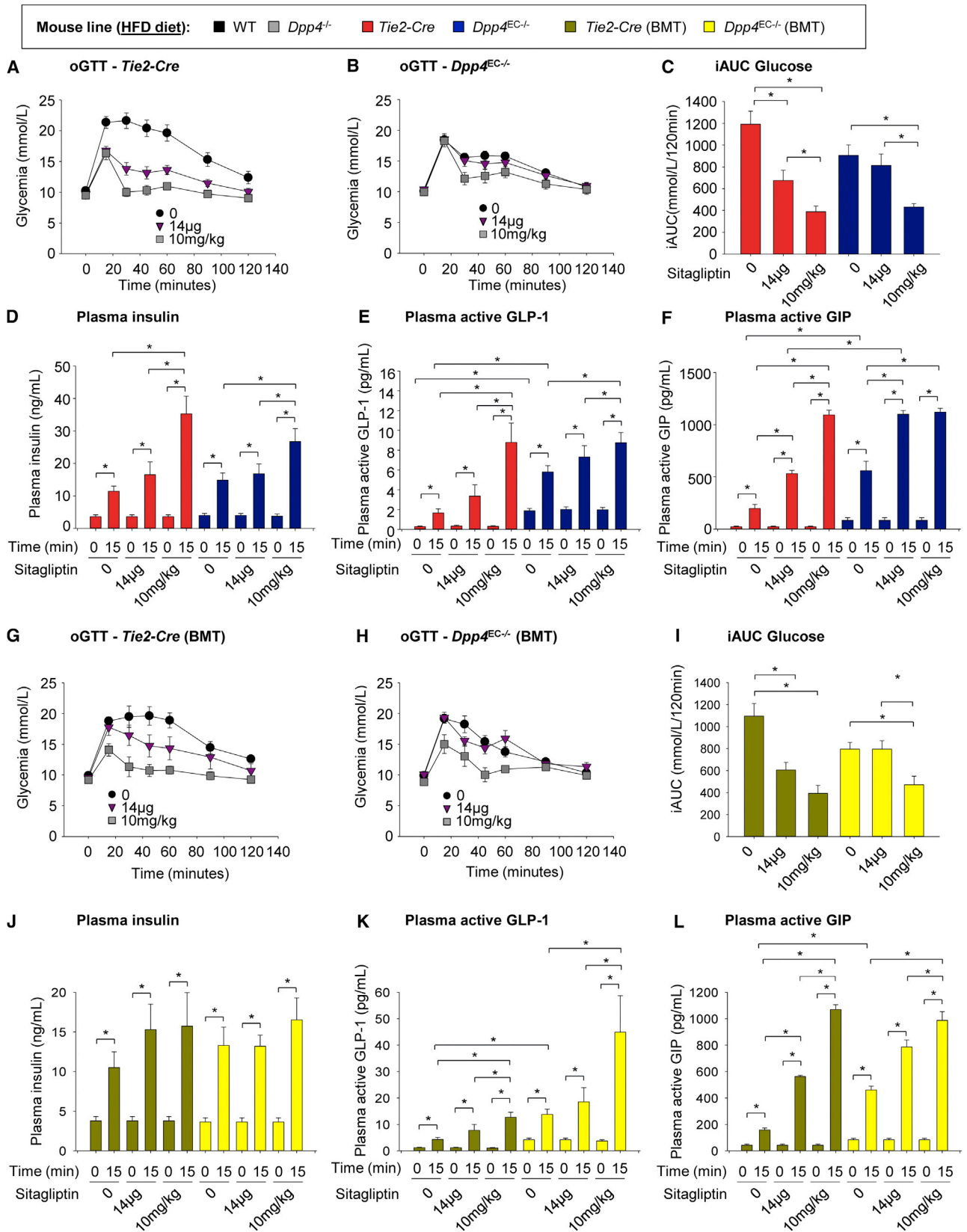
We next determined whether endothelial cell DPP4 is an important target for the glucoregulatory actions of sitagliptin. Consistent with data in WT mice (Figure 1B), *Tie2-Cre* mice exhibited a dose-dependent improvement in glucose tolerance following intestine-selective and systemic inhibition of DPP4 with sitagliptin (Figures 4H and 4I). This dose-dependent improvement in glucose tolerance in control mice was associated with increased levels of insulin, active GLP-1, and active GIP (Figures 4K-4M). In contrast, the differential glucoregulatory response to enteric versus systemic inhibition with sitagliptin was lost in $Dpp4^{EC-/-}$ mice, with maximum glucose lowering achieved with the intestinal-selective dose of sitagliptin (Figures 4I and 4J). Consistent with the glucose excursion data, both enteral and systemic DPP4 inhibition produced a further modest and similar augmen-

tation of the already elevated levels of insulin, active GLP-1, and active GIP in $Dpp4^{EC-/-}$ mice (Figures 4K-4M). Moreover, the already improved glucose tolerance (Figure 4C), in both *Tie2-Cre*(BMT) and $Dpp4^{EC-/-}$ (BMT) mice (compared to *Tie2-Cre* and $Dpp4^{EC-/-}$ mice, Figure 4B), was not further affected by intestine-selective sitagliptin treatment (Figures S6G-S6L).

HFD-Fed $Dpp4^{EC-/-}$ and $Dpp4^{EC-/-}$ (BMT) Mice Are Protected from Glucose Intolerance in the Insulin-Resistant State

As previous studies have shown that whole body $Dpp4^{-/-}$ mice are resistant to the deleterious metabolic effects of high fat feeding (Conarello et al., 2003), and this is validated in Figure S7A, we analyzed $Dpp4^{EC-/-}$ mice after 8 weeks of HFD feeding. No differences in body weight or food intake were observed in $Dpp4^{EC-/-}$ and $Dpp4^{EC-/-}$ (BMT) mice compared to their respective controls (Figures S7B-S7E).

As previously described in settings of weight gain (Lamers et al., 2011; Nagakura et al., 2003; Yang et al., 2014), plasma DPP4 activity increased in all groups after HFD-feeding (Figure 1A versus 1H), yet remained significantly lower in HFD-fed $Dpp4^{EC-/-}$ and $Dpp4^{EC-/-}$ (BMT) mice compared with controls (Figure 5A). $Dpp4^{-/-}$ mice demonstrated robust protection against glucose intolerance in response to HFD-feeding (Figure 5B). Interestingly, in contrast to the lack of improvement in



(legend on next page)

glucose control detected in regular chow-fed mice (Figures 4B and 4C), both *Dpp4*^{EC-/-} and *Dpp4*^{EC-/-}(BMT) showed a significant improvement in glucose tolerance compared to their respective controls (Figures 5C and 5D), and insulin levels were higher 15 min post-glucose administration (Figure 5E). Moreover, significant elevations in both active GLP-1 (3-fold) and active GIP (2.5-fold) were detected after oral glucose administration (Figures 5F and 5G).

We next assessed insulin action in HFD-fed control and *Dpp4*^{EC-/-} mice. Arterial glucose was clamped at similar levels in HFD-fed control and *Dpp4*^{EC-/-} mice (Figure S7F). The GIR necessary to maintain euglycemia was not different between groups (Figures S7G and S7H). In contrast to findings under chow-fed conditions, clamp insulin levels were not higher in *Dpp4*^{EC-/-} mice (Figure S7I). Insulin-mediated suppression of endoR_a was not significantly different between HFD-fed control and *Dpp4*^{EC-/-} mice (Figure S7J). The stimulation of R_d in response to insulin was also not significantly different between groups (Figure S7K).

HFD-Feeding Extinguishes the Glucoregulatory Sensitivity to Low Dose Sitagliptin in *Dpp4*^{EC-/-} and *Dpp4*^{EC-/-}(BMT) Mice

We next assessed the effects of insulin resistance on intestinal-selective DPP4 inhibition versus systemic DPP4 inhibition with sitagliptin treatment. *Tie2-Cre* control mice exhibited a proportional reduction in glycaemia to each dose of sitagliptin (Figures 6A and 6C). In contrast, intestinal-selective inhibition of DPP4 with sitagliptin had no effect on glucose tolerance in HFD-fed *Dpp4*^{EC-/-} mice whereas, systemic inhibition of DPP4 with sitagliptin improved glucose tolerance (Figures 6B and 6C). Consistent with findings in WT mice, *Tie2-Cre* control mice exhibited a significant increase in plasma levels of insulin and active GLP-1 only in response to systemic DPP4 inhibition; however, GIP was significantly elevated in response to both 14 μg of sitagliptin and systemic inhibition (Figures 6D–6F). Similarly, selective intestinal inhibition of DPP4 in *Dpp4*^{EC-/-} mice with sitagliptin did not augment levels of plasma insulin or active GLP-1 but did significantly increase active GIP levels (Figures 6D–6F). Increased plasma levels of insulin and active GLP-1 (but not active GIP) were detected following administration of the higher systemic dose of sitagliptin in *Dpp4*^{EC-/-} mice (Figures 6D–6F). Following bone marrow transplantation, control mice (*Tie2-Cre* BMT) also exhibited dose-dependent reductions in glucose excursions in response to sitagliptin administration (Figures 6G and 6I). Consistent with findings in the absence of bone marrow transplantation, high fat fed *Dpp4*^{EC-/-}(BMT) mice did not exhibit a glucoregulatory response to intestine-selective inhibition of DPP4 with sitagliptin but retained responsiveness to systemic DPP4 inhibition (Figures 6H and 6I). No differences in insulin

levels were noted between genotypes or sitagliptin doses (Figure 6J); however, *Dpp4*^{EC-/-}(BMT) mice had elevated levels of plasma active GLP-1 and GIP after oral glucose administration, in the absence of sitagliptin (Figures 6K and 6L).

DISCUSSION

Incretin hormones (i.e., GIP and GLP-1) are secreted by enteroendocrine K- and L-cells, in response to food ingestion to promote efficient nutrient disposal. The development of DPP4i was based on a classical paradigm linking systemic reduction of plasma DPP4 activity with increased circulating levels of active GLP-1 and GIP, which in turn, augment insulin and inhibit glucagon secretion and lower glucose (Deacon, 2004; Drucker, 2007; Omar and Ahrén, 2014). However, circulating levels of incretin hormones are extremely low and as little as 10% of intact bioactive GLP-1 secreted by L-cells actually reaches the pancreas (Hansen et al., 1999; Hjøllund et al., 2011). Furthermore, administration of a low dose of DPP4i to selectively inhibit DPP4 activity locally within the intestine is sufficient to improve glucose tolerance (Omar and Ahrén, 2014; Waget et al., 2011). These findings highlight the importance of a local, intestinal DPP4-sensitive enteroinsular axis for the control of glucose homeostasis. Nevertheless, the precise DPP4⁺ cell types within the gut responsible for these DPP4-dependent glucoregulatory actions have not been identified.

Enteric Inhibition of DPP4 by Sitagliptin Significantly Improves Glucose Tolerance in Chow-Fed and HFD-Fed Mice

We now reproduce the findings of Waget et al. (2011) that local intestinal DPP4 inhibition improves oral glucose tolerance in WT mice. Importantly, we extend these observations by demonstrating that the glucoregulatory actions of enteric DPP4 inhibition are completely extinguished in DIRKO mice, thereby reaffirming a dominant role for activation of both incretin receptors in the glycaemic response to DPP4 inhibition (Flock et al., 2007; Hansotia et al., 2004). Interestingly, intestinal selective DPP4 inhibition with sitagliptin was sufficient to augment circulating levels of insulin, active GLP-1 and active GIP under chow diet-fed conditions, despite no inhibition of systemic DPP4 activity. In contrast, in HFD-fed WT mice, intestinal-selective inhibition of DPP4 with sitagliptin improved glucose excursion by over 50% without a detectable increase in plasma levels of insulin, active GLP-1 and active GIP, highlighting the importance of local, enteral-portal incretin gradients (Nakajima et al., 2015; Waget et al., 2011) in the control of glucose homeostasis under these conditions. We then sought to identify the cellular origin of DPP4 within the gastrointestinal tract critical for glucoregulation and, as such, genetically eliminated *Dpp4* in enterocytes, endothelial cells, and immune cells.

Figure 6. HFD-Feeding Extinguishes the Glucoregulatory Sensitivity to Low Dose Sitagliptin in *Dpp4*^{EC-/-} and *Dpp4*^{EC-/-}(BMT) Mice

(A–C) Oral glucose tolerance in *Tie2-Cre* and *Dpp4*^{EC-/-} mice treated with 14 μg/mouse or 10 mg/kg body weight sitagliptin and fed a HFD for 4–6 weeks (n = 15–27 mice/group).

(D–F) Plasma insulin (D), active GLP-1 (E), and active GIP (F) measured at 0 and 15 min after glucose challenge (n = 8–15/group).

(G–I) Oral glucose tolerance in *Tie2-Cre* (BMT) and *Dpp4*^{EC-/-}(BMT) mice reconstituted with WT bone marrow treated with 14 μg/mouse and 10 mg/kg body sitagliptin and fed a HFD for 4–6 weeks (n = 7–8 mice/group).

(J–L) Plasma insulin (J), active GLP-1 (K), and active GIP (L) measured at 0 or 15 min after glucose challenge (n = 7–8/group). Data are presented as the mean ± SEM. *p ≤ 0.05.

DPP4 Expressed in Villin⁺ Enterocytes Does Not Contribute to Incretin Cleavage or Glucoregulation

Although enterocytes within the mucosal epithelium account for 85%–90% of total DPP4 expression in the gut, our data show that DPP4 activity in villin⁺ epithelial cells does not contribute significantly to circulating DPP4 activity and does not play an important role in the cleavage of GLP-1 and GIP. Importantly, although intestine-selective inhibition of DPP4 with sitagliptin potently reduced DPP4 activity in gut mucosal extracts (that contain predominantly enterocytes), genetic elimination of *Dpp4* in *Dpp4*^{Gut^{-/-}} mice had no effect on basal glucose tolerance and did not abrogate the glucoregulatory effects of intestinal-selective DPP4 inhibition under regular chow or HFD conditions. Hence, the principal DPP4⁺ cell type within the small bowel, the enterocyte, does not substantially contribute to DPP4-mediated control of glucose homeostasis.

Genetic Elimination of DPP4 in Tie2⁺ Cells Reveals Cellular Origin of DPP4 Responsible for Incretin Cleavage

In contrast to findings in *Dpp4*^{Gut^{-/-}} mice, DPP4 activity in the intestine of *Dpp4*^{EC^{-/-}} mice was not reduced following genetic elimination of DPP4 in vascular endothelial cells and cells of hematopoietic origin. Nevertheless, our study revealed important contributions from endothelial cells and bone marrow-derived cells to total plasma DPP4 activity (Figure 3I). Targeting DPP4 deletion in endothelial cells decreased DPP4 activity by ~25%, and bone marrow transplantation studies revealed a further contribution of hematopoietic cells to total plasma DPP4 activity, in keeping with findings reported by others (Wang et al., 2014). Consistent with the immunohistochemical localization of DPP4 in capillary endothelium adjacent to GLP-1 secreting enteroendocrine cells (Hansen et al., 1999), our genetic data demonstrated that endothelial cell DPP4 is responsible for inactivation of GLP-1 and GIP in the post-prandial state under both chow- and HFD-fed conditions. Although DPP4 is widely expressed in cells of hematopoietic origin, previous studies have not revealed a role for bone marrow-derived cells in the control of incretin inactivation. Unexpectedly, fasting plasma levels of intact GIP were reduced in *Dpp4*^{EC^{-/-}} mice after bone marrow transplantation. These findings suggest a heretofore unappreciated role for one or more hematopoietic cell lineages in the DPP4-mediated inactivation of GIP (Table S1). Nevertheless, despite a contribution of bone marrow-derived cells to plasma DPP4 activity, *Dpp4*^{EC^{-/-}} and *Dpp4*^{EC^{-/-}}(BMT) mice displayed similar increased levels of fasting and post-prandial active GLP-1 under both regular chow- and HFD-fed conditions. Hence, DPP4⁺ endothelial cells, but not bone marrow-derived cells, are critical for control of GLP-1 inactivation. These findings highlight the utility of mouse genetics for elucidating novel cellular determinants of DPP4-dependent incretin hormone degradation.

Dietary Induction of Insulin Resistance Reveals Important Roles of DPP4 in Endothelial Cells for Glucoregulation

Surprisingly, despite increased circulating levels of intact incretin hormones and an augmented insulin response to glucose, regular chow-fed *Dpp4*^{EC^{-/-}} mice did not exhibit improved glucose tolerance. These data highlight the potential importance of local

incretin signaling gradients rather than illustrate a clear endocrine mechanism for the glucoregulation mediated by DPP4 inhibition. To more comprehensively address glucose disposal and insulin sensitivity, we performed hyperinsulinemic-euglycemic clamps. Compared to controls, *Dpp4*^{EC^{-/-}} mice had significantly decreased glucose disposal complemented by a decrease in glucose production, resulting in no overall change in the glucose infusion rate. These data are consistent with our previous studies demonstrating that genetic elimination of the *Glp1r* increased muscle glucose uptake but reduced hepatic insulin sensitivity (Ayala et al., 2010). Nevertheless, low dose sitagliptin remained effective in lowering glycemic excursions after oral glucose in *Dpp4*^{EC^{-/-}} mice. Hence, under the experimental conditions in regular chow-fed mice described here, the target(s) of selective intestinal inhibition of DPP4 remains unknown.

Unexpectedly, in contrast to the lack of a glucoregulatory phenotype on a regular chow diet, both *Dpp4*^{EC^{-/-}} and *Dpp4*^{EC^{-/-}}(BMT) mice exhibited significantly improved glucose tolerance under high fat diet conditions. Further evidence for the contribution of endothelial cell DPP4 to DPP4i-mediated glucoregulation was revealed by the lack of response of both *Dpp4*^{EC^{-/-}} and *Dpp4*^{EC^{-/-}}(BMT) high fat diet-fed mice to intestinal-selective DPP4 inhibition with low dose sitagliptin. In contrast, the response to systemic inhibition of DPP4 activity with high dose sitagliptin remained intact in *Dpp4*^{EC^{-/-}} and *Dpp4*^{EC^{-/-}}(BMT) mice. High fat feeding has significant effects on many aspects of the enteroinsular axis, and discerning the biological importance of endothelial cell DPP4 under conditions of insulin resistance requires further investigations.

Resistance to Diet-Induced Obesity in *Dpp4*^{-/-} Mice Is Not Recapitulated by Targeting DPP4 Activity in Enterocytes, Endothelial Cells, or Hematopoietic Cells

Although whole body germline inactivation of the *Dpp4* gene was associated with resistance to diet-induced obesity (Figure S7) (Conarello et al., 2003), the majority of diabetic humans treated with DPP4i do not exhibit weight loss (Deacon, 2011). Furthermore, despite significant reductions in plasma DPP4 activity in regular chow- and HFD-fed *Dpp4*^{EC^{-/-}} mice, no changes in body weight or food intake were observed. Hence, despite endothelial cell DPP4 accounting for ~50% of DPP4-mediated inactivation of GLP-1, the increased plasma GLP-1 levels detected in HFD-fed *Dpp4*^{EC^{-/-}} and *Dpp4*^{EC^{-/-}}(BMT) mice were not sufficient to control body weight. These findings highlight the importance of DPP4 activity in cell types beyond ECs, as well as other DPP4 substrates that also regulate glucose metabolism and food intake (Mulvihill and Drucker, 2014), in the integrated metabolic response to genetic or pharmacological DPP4 inhibition.

In summary, we reveal that (1) enterocyte-derived DPP4 does not contribute to plasma DPP4 activity or regulate incretin degradation, and (2) inhibition of enterocyte DPP4 does not mediate the glucoregulatory properties of intestinal-selective DPP4 inhibition. DPP4 in hematopoietic cells: (1) contributes to plasma DPP4 activity, (2) selectively cleaves GIP but not GLP-1, and (3) does not contribute to glucose control. Finally, endothelial DPP4: (1) contributes to plasma DPP4 activity, (2) is responsible for degradation of both GIP and GLP-1, and (3) is the target of gut-selective inhibition of DPP4 by sitagliptin under conditions of insulin resistance and metabolic stress (Figure 7).

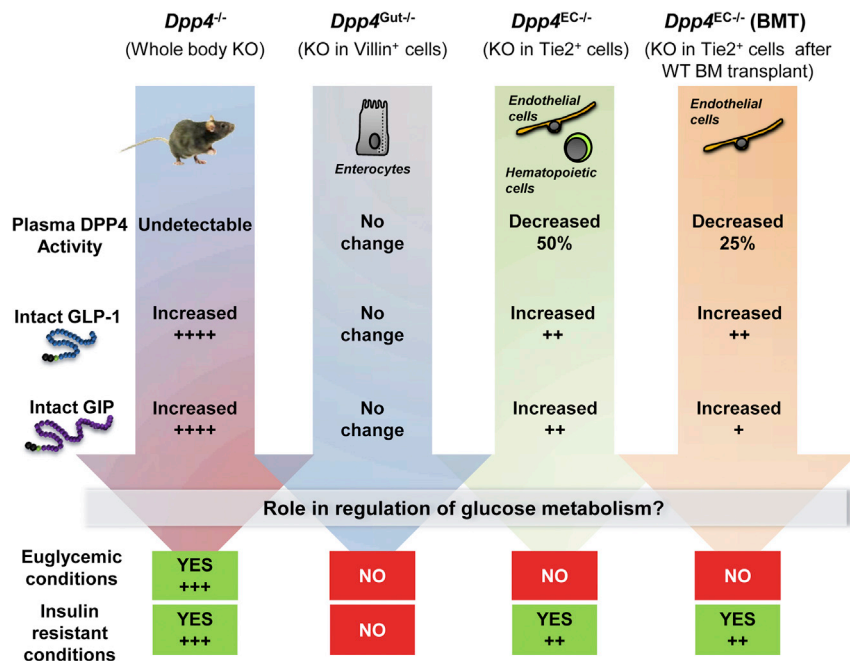


Figure 7. Role of DPP4⁺ Cell Types in the Enteroinsular Axis

Whole body genetic deletion of DPP4 increased levels of intact GIP and GLP-1 and improved glucose tolerance in both chow and HFD-fed mice. Ablation of enterocyte DPP4 in *Dpp4*^{Gut-/-} mice did not produce alterations in plasma DPP4 activity, incretin hormone levels or glucose tolerance. In contrast, endothelial cell (EC)-derived DPP4 contributed to plasma DPP4 activity, incretin degradation, and glucose control under conditions of insulin resistance. Surprisingly, DPP4⁺ cells of bone marrow origin mediated the selective degradation of fasting GIP, but not GLP-1. Collectively, these findings identify an essential role for endothelial cells but not enterocyte DPP4 in the function of the enteroinsular axis and DPP4i-mediated glucoregulation.

Interestingly, systemic DPP4 inhibition maintained glucose-lowering effects, despite genetic elimination of DPP4 within endothelial cells. This is in accordance with only partial metabolic improvement in *Dpp4*^{EC-/-} mice compared with the whole body *Dpp4*^{-/-} mice and suggests that DPP4 expression in other tissues remains critical for glucoregulation in the context of systemic DPP4 inhibition. Although treatment with DPP4i is generally well tolerated, rare adverse events including arthralgia, rhinitis, skin rash, pancreatitis, and hospitalization for heart failure have been described (Deacon, 2011; Mulvihill and Drucker, 2014). Our findings identify the importance of specific DPP4⁺ cell types for incretin degradation and glucose control under different metabolic conditions, thereby enabling targeted development of DPP4i for compartment-selective potentiation of incretin action.

EXPERIMENTAL PROCEDURES

Animals

Mice were housed under a 12-hr light/dark cycle in the Toronto Centre for Phenogenomics and maintained on regular chow (2018, 18% kcal from fat; Harlan Teklad) or HFD (45% kcal fat, 35% kcal carbohydrate, 0.05% wt/wt cholesterol, D12451, Research Diets) with free access to food and water, unless otherwise noted. *Dpp4*^{-/-} mice were re-derived from a colony described previously (Marguet et al., 2000; Sauvé et al., 2010). Double incretin receptor knockout mice (DIRKO) were previously described (Hansotia et al., 2004, 2007). Flox *Dpp4* mice were obtained from Merck Research Laboratories. The LoxP sites span the catalytic serine in exon 22 of the *Dpp4* gene. B6.Cg-Tg(Tek-cre)1Ywa/J (*Tie2-Cre*) and B6.SJL-Tg(Vil-Cre)997Gum/J (*Vil-Cre*) mice were obtained from Jackson Laboratories. As described for the B6.Cg-Tg(Tek-cre)1Ywa/J strain (de Lange et al., 2008), germline deletion was prevented by restricting *Cre* expression to male breeders. Conversely, as B6.SJL-Tg(Vil-cre)997Gum/J mice demonstrated germline deletion when *Cre* was expressed in male breeders, we restricted *Cre* expression to female breeders. To control for gene dosage, breeders were heterozygous for the *Cre* gene. Intercrossing *Cre*-positive and *Cre*-negative *Dpp4* loxP heterozygotes resulted in four genotypes: wild-type mice with no *Cre* (WT), mice

homozygous for the *LoxP* on *Dpp4* gene (Flox *Dpp4*), wild-type mice expressing *Cre* recombinase (*Tie2-Cre* and *Vil-cre*), and Flox *Dpp4* mice expressing *Cre* recombinase (*Dpp4*^{EC-/-} and *Dpp4*^{Gut-/-}). Whenever possible, we carried out experiments in all four groups of mice (Figure S3). However, due to lack of phenotypic differences in the control lines, we present data for mice expressing *Cre* and mice with the two different targeted *Dpp4* deletions. All mice were born at the expected Mendelian ratios and appeared healthy. All experiments used age- and sex-matched littermates. Mice were fasted for 5 hr prior to metabolic studies. All experiments were approved by the Animal Care and Use Subcommittee at the Toronto Centre for Phenogenomics, Mt. Sinai Hospital.

Oral and Intraperitoneal Glucose Tolerance Tests

After a 5-hr fast, mice were administered water or sitagliptin (Merck Laboratories) at 14 μg/mouse (intestinal-specific dose) or 10 mg/kg (systemic inhibition) by gavage; 30 min later regular chow-fed mice were gavaged or i.p.-injected with 20% glucose in PBS (2 g/kg of body weight). HFD-fed mice were gavaged with 50% glucose in PBS (2 g/kg of body weight). Blood for glucose measurements (Contour glucometer, Bayer Healthcare) was taken up to 120 min post-injection. Glucose tolerance was assessed using the incremental AUC glucose (iAUC). For gastric emptying, 1% acetaminophen was administered and blood samples were taken for measurement of acetaminophen (Flock et al., 2011).

Blood and Tissue Collection

Blood was taken via the tail vein during metabolic studies. For terminal studies, mice were sacrificed by CO₂ inhalation, blood was obtained by cardiac puncture. Mucosal scrapings were isolated by opening the intestine and using a surgical blade to remove the mucosal layer. Blood was collected in heparin-coated capillary microvette tubes for assessment of DPP4 activity using a fluorometric assay (substrate: 10 mM H-Gly-Pro-AMC HBr [Bachem #1-1225], standard: AMC [Bachem #Q-1025]). For measurement of active GLP-1 (Mesoscale 150JVC-1), active GIP (Crystal Chem), glucagon (Mercodia), and insulin (ultrasensitive insulin ELISA, Alpco Diagnostics) blood was mixed with 10% TED (5,000 KIU/mL Trasyolol, 1.2 mg/mL EDTA, and 0.1 nmol/L Diprotin A) and plasma stored at -80°C until the assay was performed.

Bone Marrow Transplantation

Bone marrow chimeras were generated by irradiating *Dpp4*^{EC-/-} and *Tie2-cre* CD45.2⁺ recipient male mice (1,100 cGy, split into two equal doses 4 hr apart) followed by tail vein injection of 5 × 10⁶ congenic bone marrow cells from WT B6.SJL-Ptprca Pepcb/BoyJ CD45.1⁺ male donor mice (obtained from Jackson Labs), as described (Yusta et al., 2015). After 10 weeks, the efficiency of reconstitution was assessed by flow cytometric (Gallios, Beckman Coulter) analysis of blood with CD45.1-PE-Cy5.5 and CD45.2-APC-Cy7 antibodies.

Flow Cytometry for Isolation of CD45+ and CD31+ Cells

Mice were fasted for 2 hr, injected with 25 U of heparin intramuscularly, and anesthetized with Avertin. Ice-cold DMEM was perfused through the right ventricle, and the lung was then injected with 1.5 mg of ice-cold collagenase. The lung was digested for 45 min at 37°C under constant agitation in DMEM containing collagenase type A 1.5 mg/mL, glucose 2 mg/mL, and DNase I 30 U/mL after which 25 mL of PBS containing 10% FBS was added. Lungs were pooled from two mice. Cells were strained by 40 μ M strainer and isolated by centrifugation. Red blood cells were lysed using red blood lysis solution (BioLegend) and resuspended in PBS containing 2 mM EDTA, 25 mM HEPES, and 2% FCS after isolation. Cells were blocked with CD16/32 antibody. Cells were then incubated for 30 min with fluorophore-conjugated antibodies to identify endothelial cells (APC-CD31 [551262, BD Biosciences]) and hematopoietic cells (PE-30-FIT [alpha CD45], PE-Ter119, PE-I-A/I-E [M5/114.15.2; Sunnybrook antibody core facility, Toronto, Ontario], and PE-CD41 [558040, BD Biosciences]). Target populations of live cells (DAPI-) were isolated using an Astrios MoFlo cell sorter (Beckman Coulter).

Food Intake

For calculation of food intake, mice were placed in individual cages with measured amounts of food and bedding for 72 hr.

Gene Expression

First-strand cDNA was synthesized from total RNA using the SuperScript III synthesis system (Invitrogen). Tissue mRNA levels were determined using a two-step quantitative real-time PCR protocol on an ABI Prism (model 7900 HT) Sequence Detection System (Applied Biosystems) according to the manufacturer's instructions. Primer probe sets were manufactured by TaqMan Assays-on-Demand (Applied Biosystems). The standard curve method was used to determine mRNA concentrations, and each gene was normalized to cyclophilin (*Ppia*) expression.

Hyperinsulinemic-Euglycemic Clamps

Flox *Dpp4*, *Tie2-Cre*, and *Dpp4*^{EC-/-} mice on chow or high fat diets were catheterized for at least 5 days before experimentation and clamped as described previously (Ayala et al., 2008) with some modifications as described below. Briefly, hyperinsulinemic-euglycemic clamps were performed on 5-hr fasted mice. A 2.5- μ Ci bolus of [³-³H]glucose was given at $t = -90$ min before insulin infusion, followed by a 0.04 μ Ci/min infusion for 90 min. Blood was obtained via an arterial catheter. Basal glucose-specific activity was determined from blood samples taken at $t = -15$ and -5 min. Fasting insulin levels were determined from samples taken at $t = -5$ min. The clamp was begun at $t = 0$ min with a continuous infusion of human insulin (2.5 mU/kg/min, Humulin R; Eli Lilly). Blood glucose samples were taken every 10 min starting at $t = 0$ min. A variable glucose infusion containing 50% dextrose spiked with [³-³H]glucose (0.06 μ Ci/ μ L) was administered to maintain euglycemia (~150–160 mg/dL). Mice received saline-washed erythrocytes from donors throughout the clamp (5–6 μ L/min). Blood samples (80–240 μ L) were taken every 10 min from $t = 80$ to 120 min and processed to determine plasma [³-³H]glucose. Clamp insulin was determined at $t = 100$ and 120 min. At $t = 120$ min, mice were anesthetized with sodium pentobarbital. Glucose appearance (R_a) and disappearance (R_d) were analyzed using Steele non-steady-state equations. Endogenous glucose production (endo R_a) was calculated by subtracting the glucose infusion rate from total R_a (Ayala et al., 2008).

Statistical Methods

Results are expressed as the mean \pm SEM. Statistical comparisons were made by one- or two-way ANOVA followed by Tukey post hoc or by Student's *t* test (only two conditions) using GraphPad Prism 5. Statistically significant differences are indicated as * $p \leq 0.05$.

SUPPLEMENTAL INFORMATION

Supplemental Information includes Supplemental Experimental Procedures, seven figures, and one table and can be found with this article online at <http://dx.doi.org/10.1016/j.cmet.2016.10.007>.

AUTHOR CONTRIBUTIONS

Conceptualization, E.E.M., E.M.V., and D.J.D.; Investigation, E.E.M., E.M.V., B.G., J.E.C., J.R.U., L.L.B., J.A., M.A.B., B.Y., D.M., and K.W.A.B. Formal Analysis & Visualization, E.E.M. and E.M.V.; Writing – Original Draft, E.E.M., E.M.V., and D.J.D.; Writing – Review & Editing, B.G., J.E.C., J.R.U., L.L.B., B.Y., K.W.A.B., M.A.B., J.E.A., and D.J.D. Funding Acquisition and Project Administration, D.J.D.; Resources, J.E.A. and D.J.D.; Supervision, D.J.D. and J.E.A.

ACKNOWLEDGMENTS

The authors would like to acknowledge the Centre for Modeling Human Disease (CMHD) at the Lunenfeld-Tanenbaum Research Institute as well as the Antibody core facility at Sunnybrook Research Institute for excellent technical assistance. This work was funded by grants 142395 and 123391 from the Canadian Institutes of Health Research to D.J.D. E.E.M. has received fellowship funding from the Canadian Diabetes Association and the Canadian Institutes of Health Research. E.M.V. has received fellowship funding from the Canadian Diabetes Association. J.R.U. was supported by fellowships from the Canadian Institutes of Health Research and the Alberta Innovates-Health Solutions. J.E.C. has received fellowships from the Banting and Best Diabetes Centre, University of Toronto, and the Canadian Institutes of Health Research. D.J.D. is supported by a Canada Research Chair in Regulatory Peptides and a Banting and Best Diabetes Centre-Novo Nordisk Chair in Incretin Biology. J.R.U. has received a speaker's honorarium for symposia sponsored by Novo Nordisk. D.J.D. has served as an advisor or consultant to Arisaph Pharmaceuticals, Intarcia, Merck Research Laboratories, MedImmune, Novo Nordisk, and Receptos Inc.

Received: July 5, 2016

Revised: September 6, 2016

Accepted: October 12, 2016

Published: November 10, 2016

REFERENCES

- Ayala, J.E., Bracy, D.P., Hansotia, T., Flock, G., Seino, Y., Wasserman, D.H., and Drucker, D.J. (2008). Insulin action in the double incretin receptor knockout mouse. *Diabetes* 57, 288–297.
- Ayala, J.E., Bracy, D.P., James, F.D., Burmeister, M.A., Wasserman, D.H., and Drucker, D.J. (2010). Glucagon-like peptide-1 receptor knockout mice are protected from high-fat diet-induced insulin resistance. *Endocrinology* 151, 4678–4687.
- Burcelin, R., Gourdy, P., and Dalle, S. (2014). GLP-1-based strategies: a physiological analysis of differential mode of action. *Physiology (Bethesda)* 29, 108–121.
- Campbell, J.E., and Drucker, D.J. (2013). Pharmacology, physiology, and mechanisms of incretin hormone action. *Cell Metab.* 17, 819–837.
- Conarello, S.L., Li, Z., Ronan, J., Roy, R.S., Zhu, L., Jiang, G., Liu, F., Woods, J., Zycband, E., Moller, D.E., et al. (2003). Mice lacking dipeptidyl peptidase IV are protected against obesity and insulin resistance. *Proc. Natl. Acad. Sci. USA* 100, 6825–6830.
- de Lange, W.J., Halabi, C.M., Beyer, A.M., and Sigmund, C.D. (2008). Germ line activation of the *Tie2* and *SMMHC* promoters causes noncell-specific deletion of floxed alleles. *Physiol. Genomics* 35, 1–4.
- Deacon, C.F. (2004). Therapeutic strategies based on glucagon-like peptide 1. *Diabetes* 53, 2181–2189.
- Deacon, C.F. (2011). Dipeptidyl peptidase-4 inhibitors in the treatment of type 2 diabetes: a comparative review. *Diabetes Obes. Metab.* 13, 7–18.
- Deacon, C.F., Johnsen, A.H., and Holst, J.J. (1995). Degradation of glucagon-like peptide-1 by human plasma in vitro yields an N-terminally truncated peptide that is a major endogenous metabolite in vivo. *J. Clin. Endocrinol. Metab.* 80, 952–957.

- Drucker, D.J. (2007). Dipeptidyl peptidase-4 inhibition and the treatment of type 2 diabetes: preclinical biology and mechanisms of action. *Diabetes Care* 30, 1335–1343.
- Drucker, D.J., and Nauck, M.A. (2006). The incretin system: glucagon-like peptide-1 receptor agonists and dipeptidyl peptidase-4 inhibitors in type 2 diabetes. *Lancet* 368, 1696–1705.
- Flock, G., Baggio, L.L., Longuet, C., and Drucker, D.J. (2007). Incretin receptors for glucagon-like peptide 1 and glucose-dependent insulinotropic polypeptide are essential for the sustained metabolic actions of vildagliptin in mice. *Diabetes* 56, 3006–3013.
- Flock, G., Holland, D., Seino, Y., and Drucker, D.J. (2011). GPR119 regulates murine glucose homeostasis through incretin receptor-dependent and independent mechanisms. *Endocrinology* 152, 374–383.
- Hansen, L., Deacon, C.F., Orskov, C., and Holst, J.J. (1999). Glucagon-like peptide-1-(7-36)amide is transformed to glucagon-like peptide-1-(9-36)amide by dipeptidyl peptidase IV in the capillaries supplying the L cells of the porcine intestine. *Endocrinology* 140, 5356–5363.
- Hansotia, T., Baggio, L.L., Delmeire, D., Hinke, S.A., Yamada, Y., Tsukiyama, K., Seino, Y., Holst, J.J., Schuit, F., and Drucker, D.J. (2004). Double incretin receptor knockout (DIRKO) mice reveal an essential role for the enteroinsular axis in transducing the glucoregulatory actions of DPP-IV inhibitors. *Diabetes* 53, 1326–1335.
- Hansotia, T., Maida, A., Flock, G., Yamada, Y., Tsukiyama, K., Seino, Y., and Drucker, D.J. (2007). Extrapancratic incretin receptors modulate glucose homeostasis, body weight, and energy expenditure. *J. Clin. Invest.* 117, 143–152.
- Hjollund, K.R., Deacon, C.F., and Holst, J.J. (2011). Dipeptidyl peptidase-4 inhibition increases portal concentrations of intact glucagon-like peptide-1 (GLP-1) to a greater extent than peripheral concentrations in anaesthetised pigs. *Diabetologia* 54, 2206–2208.
- Inzucchi, S.E., Bergenstal, R.M., Buse, J.B., Diamant, M., Ferrannini, E., Nauck, M., Peters, A.L., Tsapas, A., Wender, R., and Matthews, D.R.; American Diabetes Association (ADA); European Association for the Study of Diabetes (EASD) (2012). Management of hyperglycemia in type 2 diabetes: a patient-centered approach: position statement of the American Diabetes Association (ADA) and the European Association for the Study of Diabetes (EASD). *Diabetes Care* 35, 1364–1379.
- Lamers, D., Famulla, S., Wronkowitz, N., Hartwig, S., Lehr, S., Ouwens, D.M., Eckardt, K., Kaufman, J.M., Ryden, M., Müller, S., et al. (2011). Dipeptidyl peptidase 4 is a novel adipokine potentially linking obesity to the metabolic syndrome. *Diabetes* 60, 1917–1925.
- Lamont, B.J., Li, Y., Kwan, E., Brown, T.J., Gaisano, H., and Drucker, D.J. (2012). Pancreatic GLP-1 receptor activation is sufficient for incretin control of glucose metabolism in mice. *J. Clin. Invest.* 122, 388–402.
- Marguet, D., Baggio, L., Kobayashi, T., Bernard, A.M., Pierres, M., Nielsen, P.F., Ribel, U., Watanabe, T., Drucker, D.J., and Wagtmann, N. (2000). Enhanced insulin secretion and improved glucose tolerance in mice lacking CD26. *Proc. Natl. Acad. Sci. USA* 97, 6874–6879.
- Mulvihill, E.E., and Drucker, D.J. (2014). Pharmacology, physiology, and mechanisms of action of dipeptidyl peptidase-4 inhibitors. *Endocr. Rev.* 35, 992–1019.
- Nagakura, T., Yasuda, N., Yamazaki, K., Ikuta, H., and Tanaka, I. (2003). Enteroinsular axis of db/db mice and efficacy of dipeptidyl peptidase IV inhibition. *Metabolism* 52, 81–86.
- Nakajima, S., Hira, T., and Hara, H. (2015). Postprandial glucagon-like peptide-1 secretion is increased during the progression of glucose intolerance and obesity in high-fat/high-sucrose diet-fed rats. *Br. J. Nutr.* 113, 1477–1488.
- Nauck, M.A., and Meier, J.J. (2016). The incretin effect in healthy individuals and those with type 2 diabetes: physiology, pathophysiology, and response to therapeutic interventions. *Lancet Diabetes Endocrinol.* 4, 525–536.
- Omar, B., and Ahrén, B. (2014). Pleiotropic mechanisms for the glucose-lowering action of DPP-4 inhibitors. *Diabetes* 63, 2196–2202.
- Rolin, B., Deacon, C.F., Carr, R.D., and Ahrén, B. (2004). The major glucagon-like peptide-1 metabolite, GLP-1-(9-36)-amide, does not affect glucose or insulin levels in mice. *Eur. J. Pharmacol.* 494, 283–288.
- Sandoval, D.A., and D'Alessio, D.A. (2015). Physiology of proglucagon peptides: role of glucagon and GLP-1 in health and disease. *Physiol. Rev.* 95, 513–548.
- Sauvé, M., Ban, K., Momen, M.A., Zhou, Y.-Q., Henkelman, R.M., Husain, M., and Drucker, D.J. (2010). Genetic deletion or pharmacological inhibition of dipeptidyl peptidase-4 improves cardiovascular outcomes after myocardial infarction in mice. *Diabetes* 59, 1063–1073.
- Smith, E.P., An, Z., Wagner, C., Lewis, A.G., Cohen, E.B., Li, B., Mahbod, P., Sandoval, D., Perez-Tilve, D., Tamarina, N., et al. (2014). The role of β cell glucagon-like peptide-1 signaling in glucose regulation and response to diabetes drugs. *Cell Metab.* 19, 1050–1057.
- Tang, Y., Harrington, A., Yang, X., Friesel, R.E., and Liaw, L. (2010). The contribution of the Tie2+ lineage to primitive and definitive hematopoietic cells. *Genesis* 48, 563–567.
- Tatarkiewicz, K., Sablan, E.J., Polizzi, C.J., Villescascz, C., and Parkes, D.G. (2014). Long-term metabolic benefits of exenatide in mice are mediated solely via the known glucagon-like peptide 1 receptor. *Am. J. Physiol. Regul. Integr. Comp. Physiol.* 306, R490–R498.
- Utzschneider, K.M., Tong, J., Montgomery, B., Udayasankar, J., Gerchman, F., Marcovina, S.M., Watson, C.E., Ligueros-Saylan, M.A., Foley, J.E., Holst, J.J., et al. (2008). The dipeptidyl peptidase-4 inhibitor vildagliptin improves beta-cell function and insulin sensitivity in subjects with impaired fasting glucose. *Diabetes Care* 31, 108–113.
- Waget, A., Cabou, C., Masseboeuf, M., Cattan, P., Armanet, M., Karaca, M., Castel, J., Garret, C., Payros, G., Maida, A., et al. (2011). Physiological and pharmacological mechanisms through which the DPP-4 inhibitor sitagliptin regulates glycemia in mice. *Endocrinology* 152, 3018–3029.
- Wang, Z., Grigo, C., Steinbeck, J., von Hörsten, S., Amann, K., and Daniel, C. (2014). Soluble DPP4 originates in part from bone marrow cells and not from the kidney. *Peptides* 57, 109–117.
- Yang, F., Zheng, T., Gao, Y., Baskota, A., Chen, T., Ran, X., and Tian, H. (2014). Increased plasma DPP4 activity is an independent predictor of the onset of metabolic syndrome in Chinese over 4 years: result from the China National Diabetes and Metabolic Disorders Study. *PLoS ONE* 9, e92222.
- Yusta, B., Baggio, L.L., Koehler, J., Holland, D., Cao, X., Pinnell, L.J., Johnson-Henry, K.C., Yeung, W., Surette, M.G., Bang, K.W., et al. (2015). GLP-1R agonists modulate enteric immune responses through the intestinal intraepithelial lymphocyte GLP-1R. *Diabetes* 64, 2537–2549.

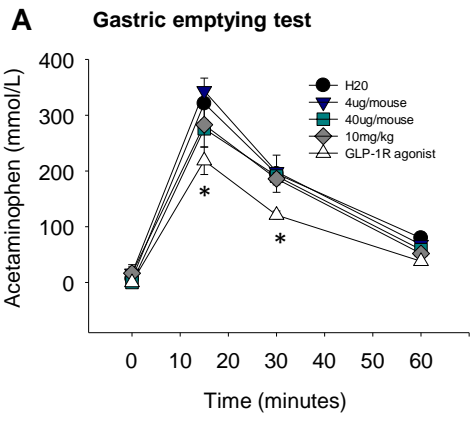
Cell Metabolism, Volume 25

Supplemental Information

**Cellular Sites and Mechanisms Linking Reduction
of Dipeptidyl Peptidase-4 Activity to Control
of Incretin Hormone Action and Glucose Homeostasis**

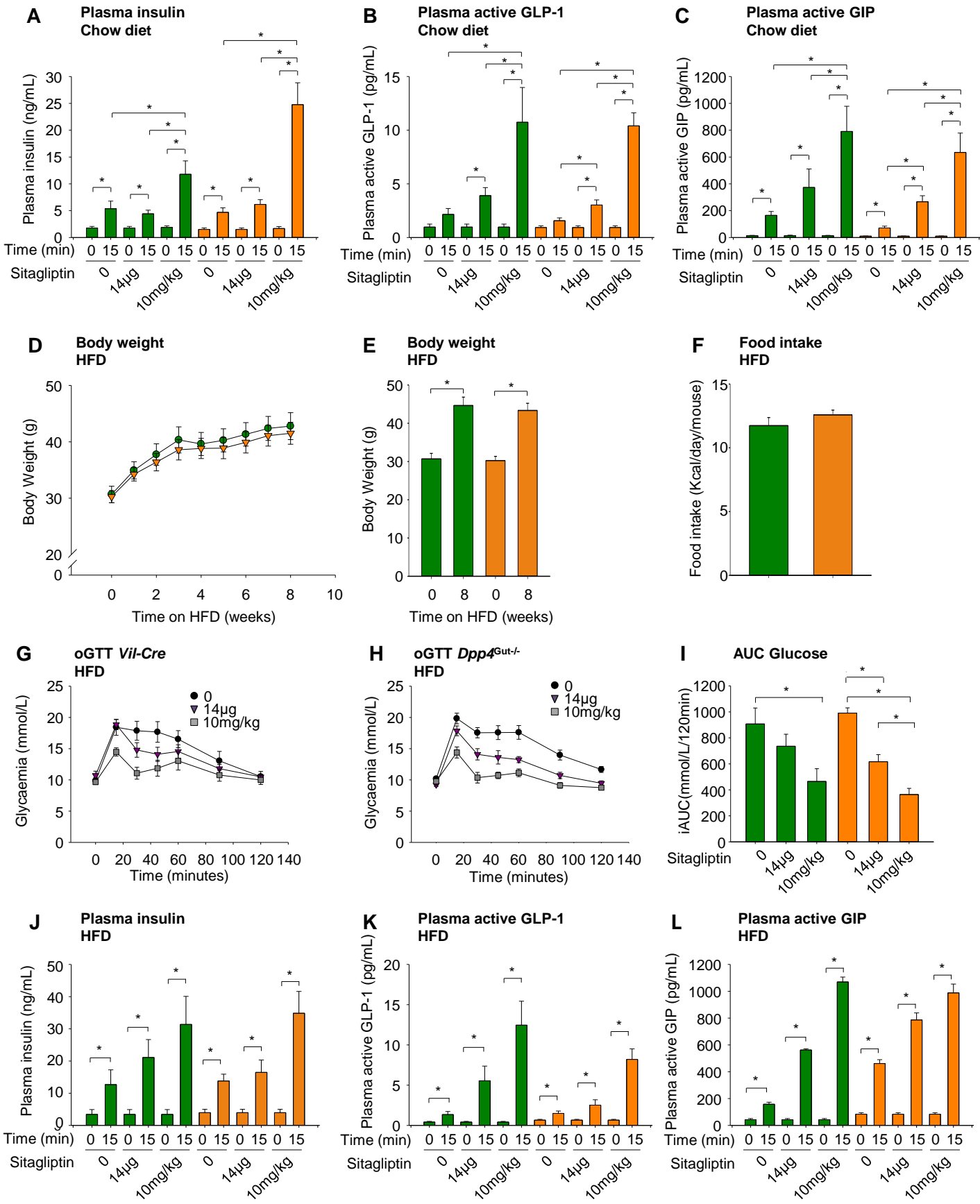
Erin E. Mulvihill, Elodie M. Varin, Bojana Gladanac, Jonathan E. Campbell, John R. Ussher, Laurie L. Baggio, Bernardo Yusta, Jennifer Ayala, Melissa A. Burmeister, Dianne Matthews, K.W. Annie Bang, Julio E. Ayala, and Daniel J. Drucker

Supplemental Figure 1

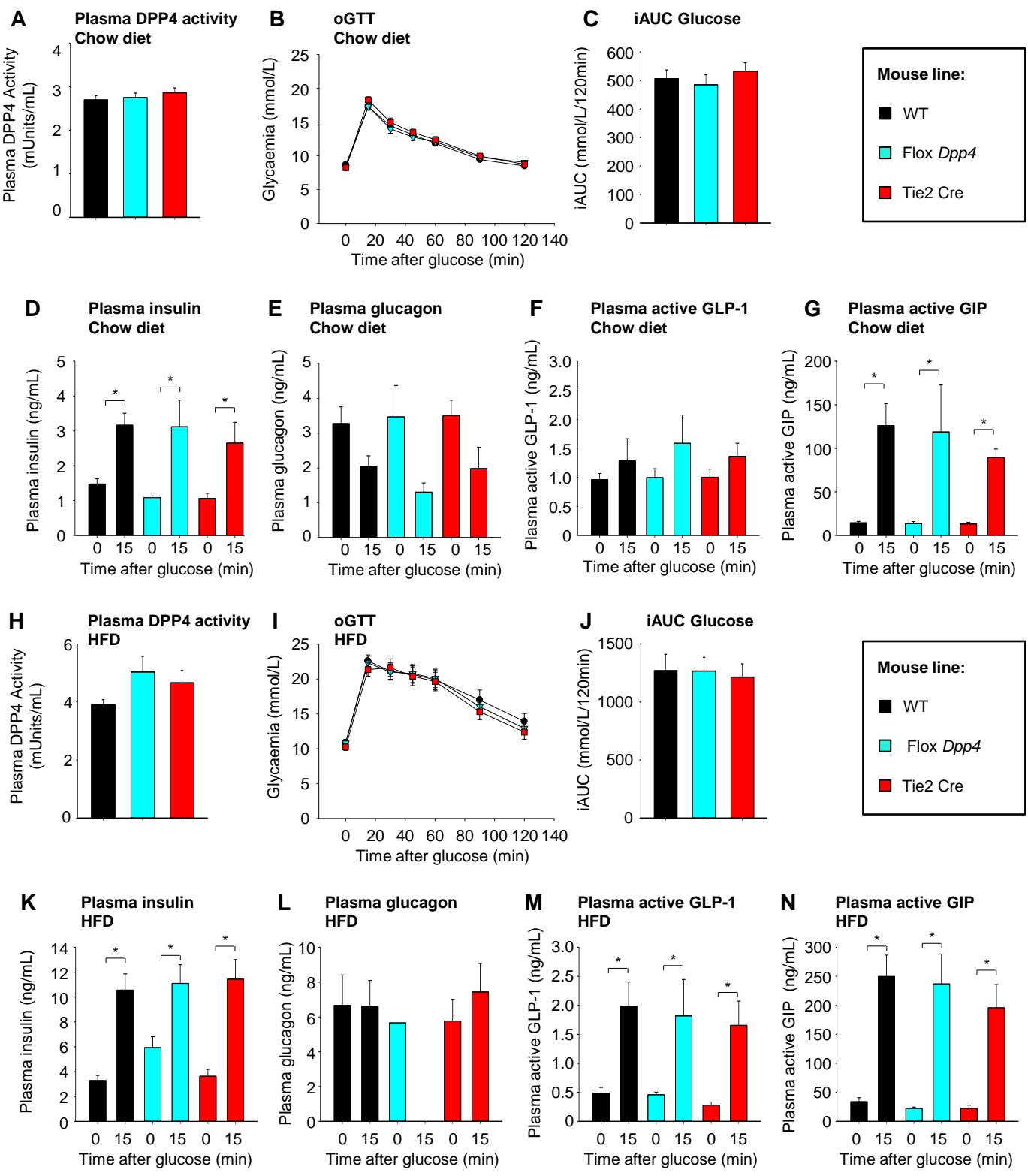


Supplemental Figure 2

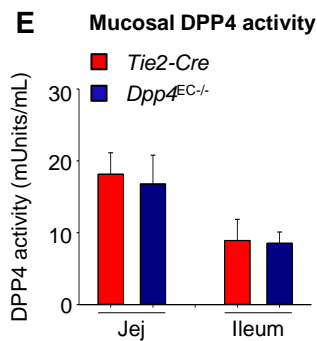
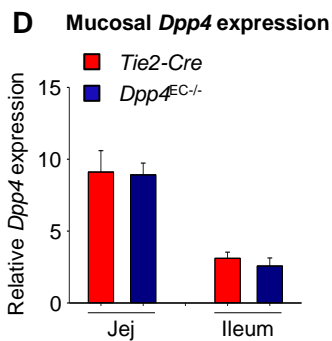
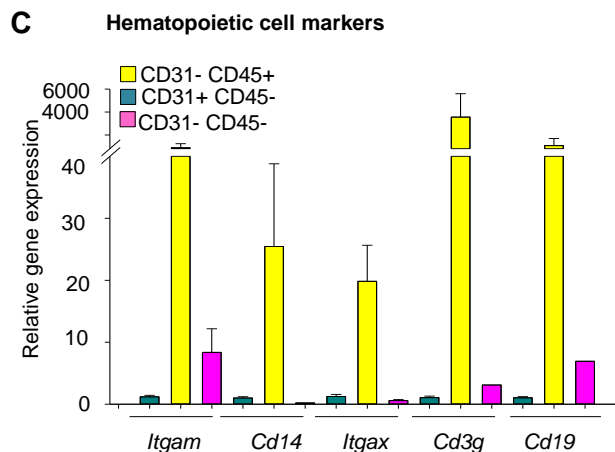
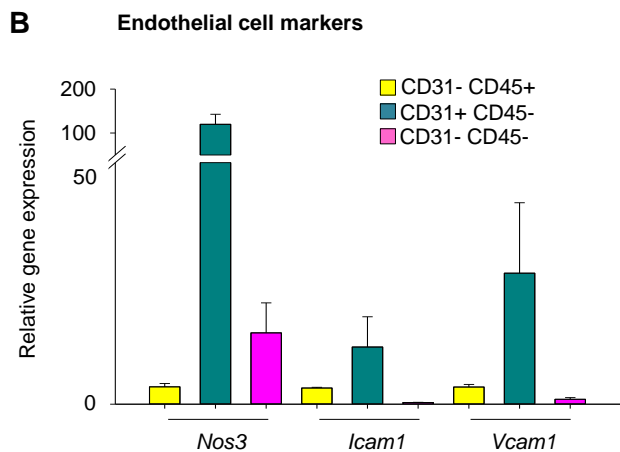
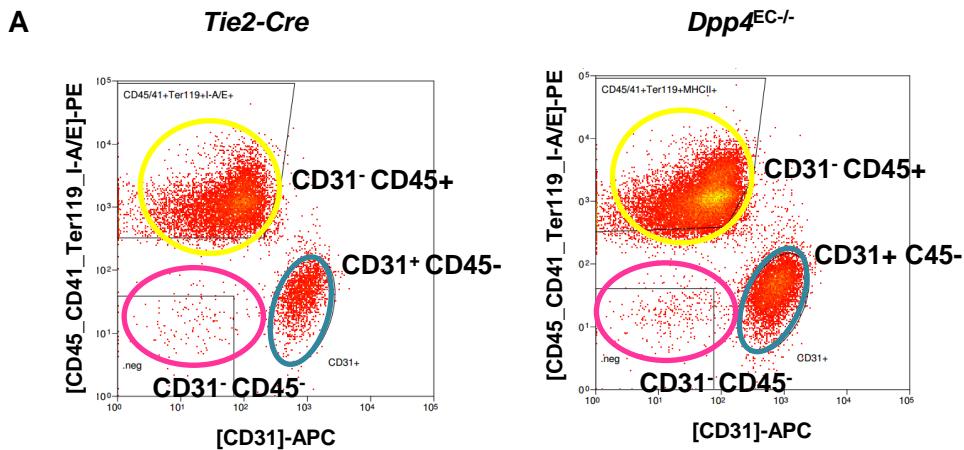
Mouse line : ■ *Vil-cre* ■ *Dpp4^{Gut-/-}*



Supplemental Figure 3

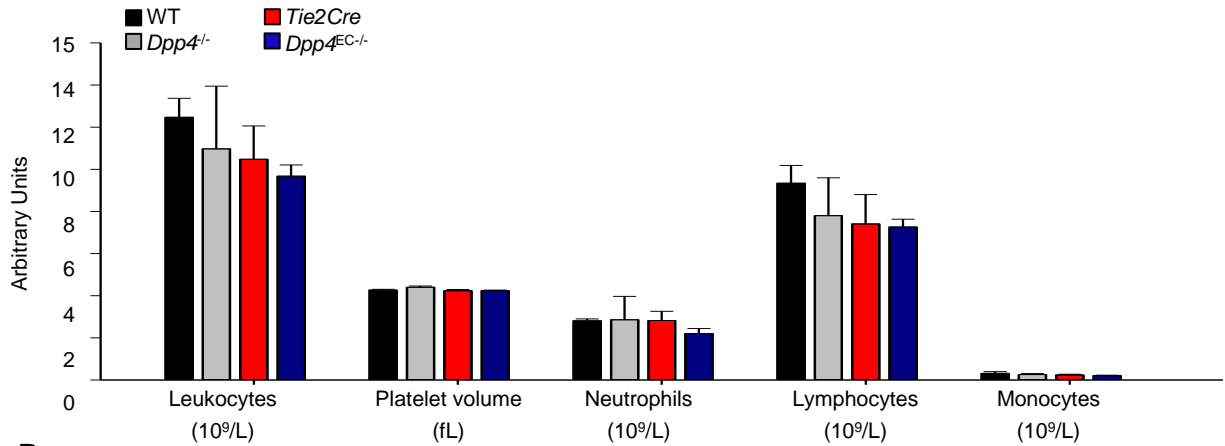


Supplemental Figure 4

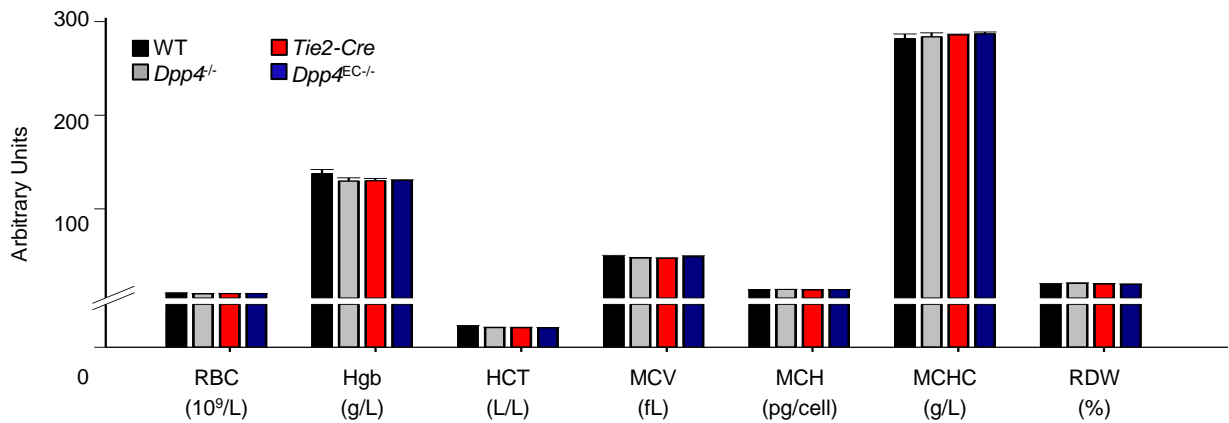


Supplemental Figure 5

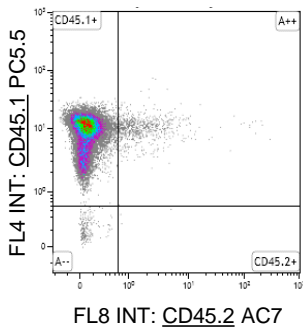
A Blood cell composition



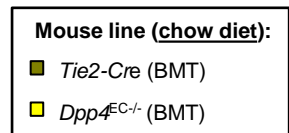
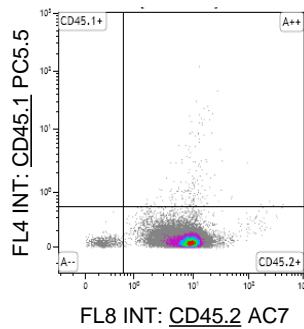
B Indices of Red Blood Cells



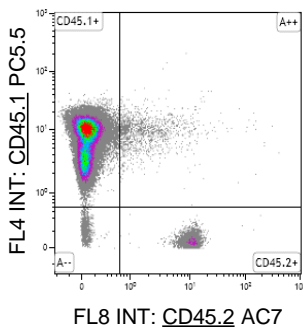
C Bone marrow donor: WT Pepboy CD45.1



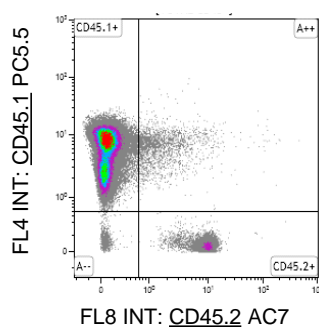
D Control mice: WT C56BL/6J CD45.2



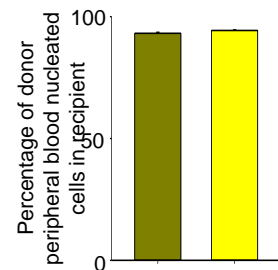
E Bone marrow recipient: *Tie2-cre* CD45.2 reconstituted with WT Pepboy CD45.1 BM (*Tie2-cre* (BMT))



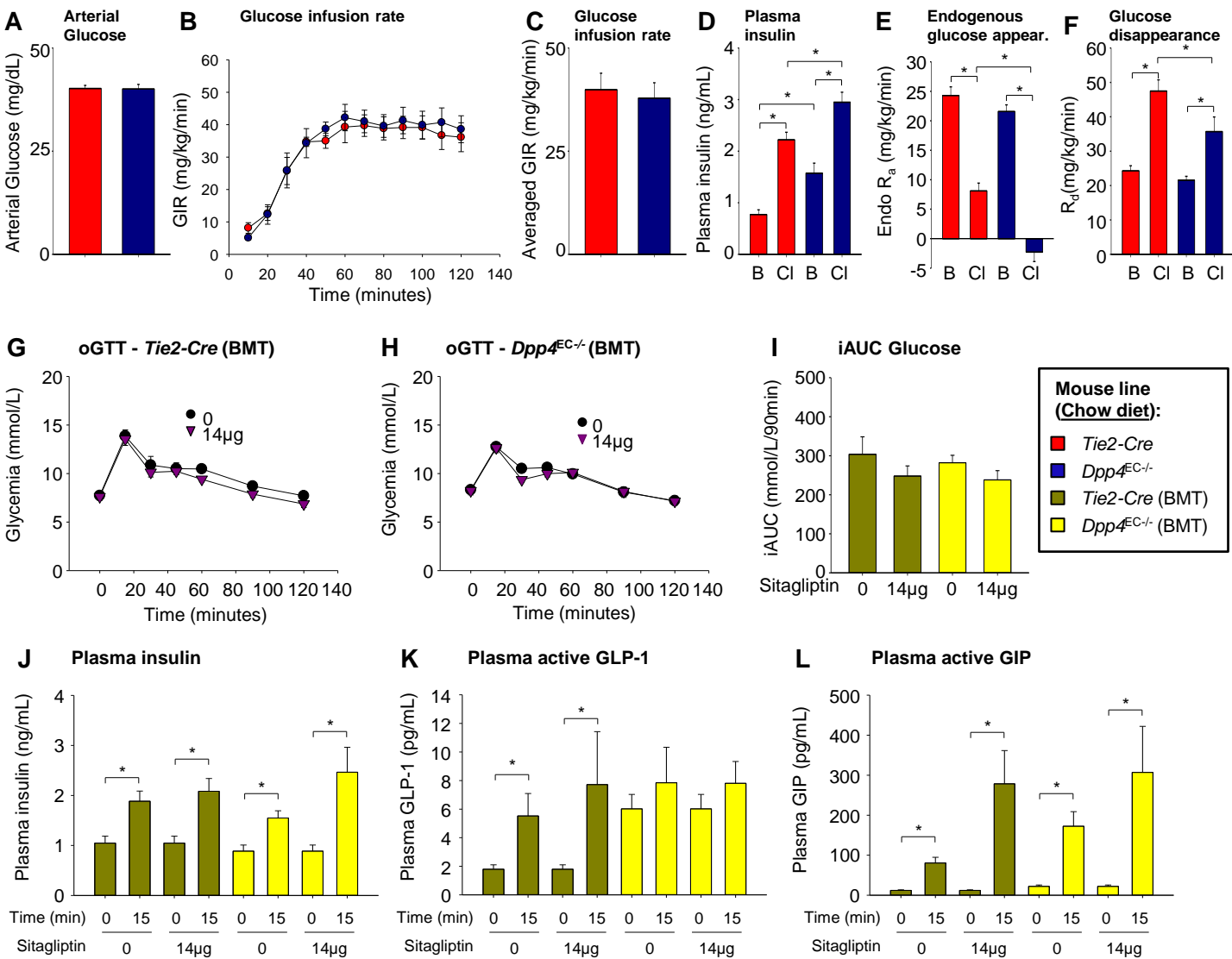
F Bone marrow Recipient: *Dpp4*^{EC-/-} CD45.2 reconstituted with WT Pepboy CD45.1 BM (*Dpp4*^{EC-/-} (BMT))



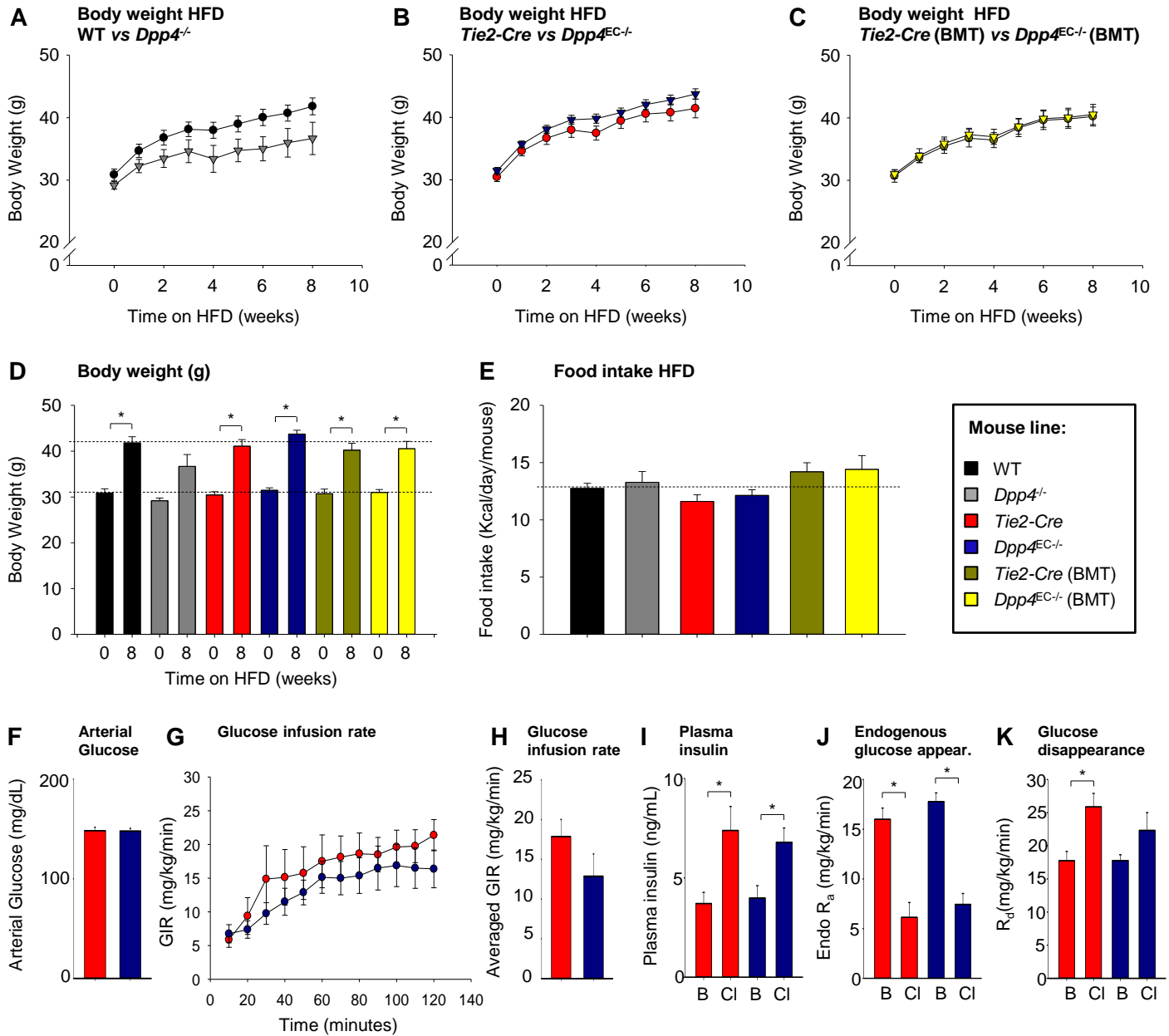
G WT donor chimerism in peripheral blood cells from *Tie2-Cre* and *Dpp4*^{EC-/-} BM recipients



Supplemental Figure 6



Supplemental Figure 7



Supplemental Table 1

Table 1 Intact plasma GIP measured in fasting and post-prandial states

		WT	<i>Dpp4</i> ^{-/-}	<i>Tie2Cre</i>	<i>Dpp4</i> ^{EC-/-}	<i>Tie2Cre</i> (BMT)	<i>Dpp4</i> ^{EC-/-} (BMT)
Fasting State	Plasma Active GIP (pg/mL)	15.5±1.9	45.2±6.7	14.8±2.5	42.6±9.5	12.1±1.4	22.1±3.5
	Intact GIP (% of <i>Dpp4</i> ^{-/-})		100%		94%		49%
Chow Diet 15 minutes Post-Glucose	Plasma Active GIP (pg/mL)	126.1±25.3	506.4±192.2	89.5±9.8	251.9±31.8	80.5±14.2	172.5±36.3
	Intact GIP (% of <i>Dpp4</i> ^{-/-})		100%		50%		34%
High Fat Diet 15 minutes Post-Glucose	Plasma Active GIP (pg/mL)	249.8±36.7	1293.5±54.9	195.8±40	560.1±89.6	157.8±16.3	461.6±36.4
	Intact GIP (% of <i>Dpp4</i> ^{-/-})		100%		44%		35%

Supplemental Figure 1 related to Main Figure 1: In contrast to treatment with a GLP-1R agonist, sitagliptin treatment did not modify gastric emptying in WT mice.

A. Plasma acetaminophen measured 0-60 minutes after administration of oral glucose mixed with 1% acetaminophen in 10 week old WT mice treated dose-dependently with sitagliptin (0, 14 μ g / mouse, 40 μ g / mouse, or 10mg/kg) or a GLP-1R agonist (Albiglutide, 2mg/kg). Data are presented as the mean \pm SEM. (n=4 mice per group). * $P \leq 0.05$ for control-treated vs. albiglutide-treated mice.

Supplemental Figure 2 related to Main Figure 2: Metabolic consequences of eliminating

Dpp4 in Villin+ cells of the gut epithelium. A-C. Plasma insulin (A), active GLP-1 (B) and active GIP (C) measured at 0 and 15 minutes after glucose challenge and 45 minutes after sitagliptin gavage during an OGTT in *Vil-Cre* or *Dpp4*^{Gut^{-/-}} mice fed on chow diet (n=4-15/per group). **D,E.** Body weight of *Vil-Cre* and *Dpp4*^{Gut^{-/-}} over 8 weeks on HFD (n=10 *Vil-Cre* and 14 *Dpp4*^{Gut^{-/-}}). **F.** Food intake expressed as average kilocalories consumed/mouse/day on HFD (n=6-13 mice/group). **G-L.** Oral glucose tolerance in *Vil-Cre* or *Dpp4*^{Gut^{-/-}} mice treated with 14 μ g/mouse or 10 mg/kg body weight sitagliptin and fed a HFD for 4-6 weeks. **G-I.** Blood glucose and area under the curve analysis taken 0-120 minutes after administration of oral glucose (n=9-14 mice/group). **J-L.** Plasma insulin (J), active GLP-1 (K) and active GIP (L) measured at 0 and 15 minutes after glucose challenge (n=5-19/group). Data are presented as the mean \pm SEM. * $P \leq 0.05$.

Supplemental Figure 3 related to Main Figure 3: Wildtype, Flox and *Tie2-Cre* mice have similar control of the enteroinsular axis under chow or high fat diet conditions.

A. DPP4 activity in plasma of chow fed 8-12 weeks-old male WT, Flox *Dpp4* and *Tie2-Cre* mice (n=19-22 mice/group). **B-C.** Blood glucose taken 0-120 minutes after administration of oral glucose and iAUC analysis of glucose excursions in chow fed 8-12 week-old male control mice fasted for 5 hours (n=30-44 mice/group). **D-G.** Plasma insulin (D), glucagon (E), active GLP-1 (F) and active GIP (G) measured at 0 and 15 minutes after glucose challenge during an OGTT in chow fed 8-12 week-old male mice (n=4-14/group). **H.** DPP4 activity in plasma of mice fed a HFD for 8 weeks (n=8-21/group). **I,J.** Blood glucose taken 0-120 minutes after administration of

oral glucose and iAUC analysis for glucose excursions in control mice fed a HFD for 4-6 weeks and fasted for 5 hours (n=14-24 mice/group). **K-N.** Plasma insulin (K), glucagon (L), active GLP-1 (M) and active GIP (N) measured at 0 and 15 minutes after glucose challenge during an OGTT in control groups of mice fed a HFD for 4-6 weeks and fasted for 5 hours (n=4-13/group). Data are presented as the mean \pm SEM. * $P \leq 0.05$.

Supplemental Figure 4 related to Main Figure 3: Phenotypic characterization of populations of CD31⁺CD45⁻, CD31⁻CD45⁺ and CD31⁻CD45⁻ cells isolated from lung and purified through flow cytometric cell sorting and DPP4 mucosal expression and activity.

A. Representative dot plots showing the gating of cell populations: CD31⁺CD45⁻ cells (endothelial cells), CD31⁻CD45⁺ cells (hematopoietic cells, including CD41⁺Ter119⁺I-A/I-E⁺ cells) and CD31⁻CD45⁻ cells (remaining cells) isolated from lung after collagenase digestion in *Tie2-Cre* or *Dpp4*^{EC-/-}. **B.** Relative mRNA expression of markers of endothelial cells to validate CD31⁺CD45⁻, CD31⁻CD45⁺ and CD31⁻CD45⁻ sorted cell populations (hematopoietic cells used for normalization) (n=2-4/group) in pooled *Tie2-Cre* and *Dpp4*^{EC-/-} mice. **C.** Relative mRNA expression of markers of hematopoietic cells to validate CD31⁺CD45⁻ and CD31⁻CD45⁺ FACS sorted cell populations (endothelial cells used for normalization) (n=2-4/group). **D.** mRNA abundance of *Dpp4* normalized to *Ppia* in mucosal scrapings of chow fed 8-12 week-old female mice (n=4-6/group). **E.** DPP4 activity in extracts from intestinal mucosal scrapings from 8-12 week-old female mice (n=3/group). Data are presented as the mean \pm SEM. Jej, Jejunum.

Supplemental Figure 5 related to Main Figure 4: Targeting of *Dpp4* in hematopoietic and endothelial cells does not alter blood counts or indices of red blood cells allowing efficient WT donor chimerism in peripheral blood cells from *Tie2-Cre* and *Dpp4*^{EC-/-} BM recipients

A,B. Results of complete blood count and indices of red blood cells from blood samples isolated from the tail vein of fed mice (n=3-8 mice/group). **C-F.** Representative dot plots showing the gating of cell populations CD45.1⁺ and CD45.2⁺ in WT Pepboy CD45.1 (C), WT C57BL/6J CD45.2 mice (D), or *Tie2-Cre* (E) and *Dpp4*^{EC-/-} BM recipients (F) 10 weeks after reconstitution. **G.** Quantitation of WT donor chimerism in peripheral blood cells from *Tie2-Cre* and *Dpp4*^{EC-/-} BM recipients. Data are presented as the mean \pm SEM. RBC = red blood cell, Hgb= hemoglobin, HCT= hematocrit, MCV = Mean corpuscular volume, MCH = mean

corpuscular hemoglobin, MCHC= mean corpuscular hemoglobin concentration and RDW= Red cell distribution width. BM= Bone Marrow.

Supplemental Figure 6 related to Main Figure 4: Hyperinsulinemic-Euglycemic Clamps in chow-fed *Tie2-Cre* and *Dpp4*^{EC/-} mice and metabolic response to sitagliptin in *Tie2-Cre* (BMT) and *Dpp4*^{EC/-} (BMT). **A-F.** Hyperinsulinemic-euglycemic clamps in 5 hours-fasted, conscious, unrestrained chow-fed control and *Dpp4*^{EC/-} mice (n=7-11 mice/group). **A.** Arterial glucose levels, **B-C.** Glucose infusion rate **D.** Plasma insulin, **E.** Basal glucose appearance (appear; Ra). **F.** Basal glucose disappearance (Rd). **G-I.** Blood glucose and area under the curve analysis taken 0-120 minutes after administration of oral glucose with and without low dose sitagliptin in regular chow-fed *Tie2-Cre* (BMT) and *Dpp4*^{EC/-} (BMT) mice (n=7-8/group). **J-L.** Plasma insulin (J), active GLP-1 (K) and active GIP (L) measured at 0 and 15 minutes after glucose challenge during an OGTT in regular chow-fed *Tie2-Cre* (BMT) and *Dpp4*^{EC/-} (BMT) mice treated with or without 14 µg/mouse sitagliptin (n=7-8/group). Data are presented as the mean ± SEM. * $P \leq 0.05$

Supplemental Figure 7 related to Main Figure 5: Body weight and food intake under chow and HFD conditions in global vs. tissue-specific *Dpp4* knockout mice and Hyperinsulinemic-Euglycemic Clamps in HFD-fed *Tie2-Cre* and *Dpp4*^{EC/-} mice.

A-C. Body weight of *Dpp4* targeted and respective control mice over 8 weeks on HFD (n=8-27 mice/group). **D.** Body weight before and 8 weeks after starting HFD in *Dpp4* targeted and respective control mice (n=8-27 mice/group). **E.** Food intake expressed as average kilocalories consumed per mouse per day (n=8-22 mice/group). **F-K.** Hyperinsulinemic-euglycemic clamps in 5 hours-fasted, conscious, unrestrained HFD-fed control and *Dpp4*^{EC/-} mice (n=7-11 mice/group). **F.** Arterial glucose levels, **G,H.** Glucose infusion rate **I.** Plasma insulin, **J.** Basal glucose appearance (appear; Ra). **K.** Basal glucose disappearance (Rd). Data are presented as the mean ± SEM. * $P \leq 0.05$.

Supplemental Table 1 related to Main Figure 7: Characterization of Intact GIP concentrations in plasma collected under fasting conditions and in response to glucose.